Comprehensive analysis of CdS / In_2S_3 / ZnS buffer layers on the performance of CIGS solar cell

A thesis submitted to the Department of Electrical, Electronic and Communication Engineering (EECE)

MIST

In partial fulfillment of the requirements

For the degree of

BACHELOR OF SCIENCE IN ELECTRICAL, ELECTRONIC AND COMMUNICATION ENGINEERING

DECEMBER, 2017

By

Mehedi Hasan (201416034)

Muhaiminul Islam (201416089)

Arif Hasan Khan (201416102)

Supervised By

Md. Kawsar Alam, Ph.D.
Associate Professor
Dept. of EEE, BUET
Dhaka-1205, Bangladesh

CERTIFICATION OF APPROVAL

The thesis titled as *"Comprehensive Analysis of CdS / In_2S_3 / ZnS buffer layers on the performance of CIGS solar cell"* submitted by Mehedi Hasan (201416034), Muhaiminul Islam (201416089) and Arif Hasan Khan (201416102) has been accepted as satisfactory in partial fulfillment of the requirement of the degree of BACHELOR OF SCIENCE IN ELECTRICAL, ELECTRONIC AND COMMUNICATION ENGINEERING on 20 December, 2017.

APPROVAL OF THE SUPERVISOR

Md. Kawsar Alam, Ph.D.
Associate Professor
Dept. of EEE, BUET
Dhaka-1205, Bangladesh

DECLARATION

It is hereby declared that this thesis or any part of it has not been submitted elsewhere for the award of any degree or diploma.

Authors

Mehedi Hasan	Muhaiminul Islam	Arif Hasan Khan
(ID: 201416034)	(ID: 201416089)	(ID: 201416102)

ACKNOWLEDGEMENTS

We would like to express our sincere gratitude to our advisor Associate Professor Dr. Md. Kawsar Alam for entrusting this project to us. We would like to thank him for many insightful conversations and for his patience in teaching us, without which we would never have finished our thesis successfully. He is actively involved in the work of all his students. We would also like to thank our department, EECE dept. MIST, for giving us opportunity to work with such a great mind of our country and giving us support in every aspects. We would like to thank our family and friends who have been instrumental in our thesis.

ABSTRACT

Thin-film solar cells (TFSCs) have the potential to reach cost effective photovoltaic generated electricity. Cadmium Sulfide (CdS), Indium Sulfide (In_2S_3) and Zinc Sulfide (ZnS) buffer layer based Copper Indium Gallium Selenide (CIGS) solar cell offers higher efficiency with low manufacturing cost. Therefore, this thesis presents a comparative study among CdS, In_2S_3 or ZnS buffer layer based CIGS solar cell. The numerical study has been performed using a Solar Cell Capacitance Simulator named SCAPS-1D. The performance of CIGS solar cell is observed by adjusting the buffer layer thickness of each CdS, In_2S_3 and ZnS. The efficiency of CdS/CIGS solar cell is found 23.74% that is higher than the efficiency of In_2S_3/CIGS (23.39%) solar cell for 50 nm buffer layer thickness. This efficiency was increased further by using ZnS/CIGS structure that corresponding to an efficiency of 25.51%. It is also found that, the increase in buffer layer thickness from the optimum level degrades the performance of CdS/CIGS and ZnS/CIGS solar cells as compared to In_2S_3/CIGS solar cell. Therefore, In_2S_3 or ZnS based CIGS cell could be an ideal candidate as a substitute of toxic CdS buffer layer based CIGS solar cell.

Table of Contents

CHAPTER 3: RESULTS AND DISCUSSIONS

CHAPTER 4: CONCLUSION

List of figures

List of Tables

LIST OF ACRONYMS AND ABBREVIATIONS

- CdS cadmium Sulfide
- ZnS zinc Sulfide
- In_2S_3 Indium Sulfide
- CIGS copper indium gallium di-selenide, $Cu(In,Ga)Se_2$
- eV electron volt
- E_g band gap energy
- Ga gallium
- J_{SC} short circuit current density
- IV current vs. voltage
- iZnO intrinsic zinc oxide
- Mo molybdenum
- Si silicon
- V_{OC} open circuit voltage
- ZnO zinc oxide
- SLG soda lime glass
- TCO transparent conducting oxide
- ε_r relative permittivity
- χ_e electron affinity
- N_c density of states in the conduction band
- N_v density states in the valence band
- μ_n electron band mobility
- μ_p hole band mobility

This page is intentionally left blank

Chapter-1
INTRODUCTION

Harvesting of sunlight is not new to life on earth. It can be said without any doubt that the entire life on the planet earth is dependent on the solar energy. Everyone might be aware of the fact that chlorophyll the green pigment in leaves and algae uses sunlight in photosynthesis and is at the bottom of the food chain. One notable point to mention here about the sunlight is that about 90% of the conversion of CO2 to O2 is done by algae and plants with the help of solar energy. One can, therefore, undoubtedly say that energy from sunlight is the driving force of our survival.

1.1 World Energy

In the modern world, growth is synchronized with energy demand. According to the IEO Report 2011 [1], the world energy consumption is prominent to rise from 505 quadrillion Btu in 2008 to 619 quadrillion Btu in 2020 and may reach 720 quadrillion Btu by 2035. Out of the 505 quadrillion Btu produced in 2008, liquid fossil fuels such as crude oil contribute 35%, coal contributes 27%,natural gas contributes 23%, 10% is contributed by renewables which include hydro, wind, solar etc., and the rest by nuclear power.

The fossil fuels including crude oil, coal and natural gas together provide around 80% of energy consumed around the world today. These fossil fuels are fast depleting and take millions of years to restock. According to some reports both the crude oil and coal are about to cross or may have already crossed their peak production [2]. These fossil fuels are not only depleting but are also emitting large amounts of so called greenhouse gases which are responsible in part for global warming [3]. The figure: 1-1 shows the increase in CO_2 in earth's atmosphere with respect to time.

Nuclear energy, which appeared to be a durable source of energy, is associated with setbacks such as complexity in waste disposal, limited availability of the nuclear raw materials like uranium, thorium etc and socio environmental hazards involved in extracting them [4]. The nuclear plant accidents like core meltdown and subsequent radiation leak at Fukushima Diiachi Nuclear Plant in Japan after being struck by a tsunami in 2011 have resulted in opposition of future nuclear establishments. Some of the OECD countries such as Germany have agreed to shut down their nuclear plants by 2020 [5].

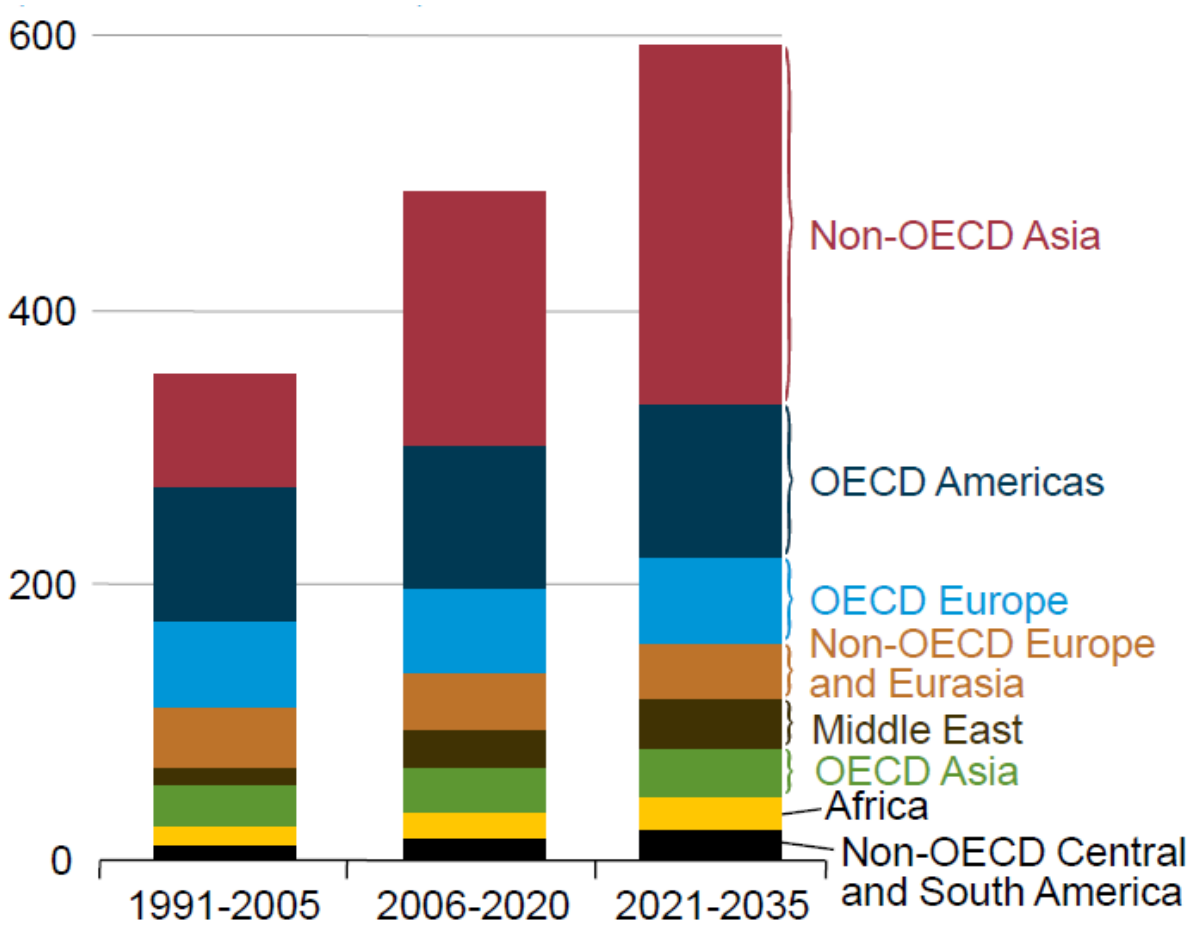

Figure 1-1: Cumulative Carbon di oxide emission in different region

Enormous availability and ecofriendly nature make renewables, the most viable alternate in all the energy sources. Here, renewables consist of wind, solar, tidal, geothermal etc. High EROEI ratio (energy returned on energy invested) is an etiquette in the energy industry. The amount of energy used for installation and operation should always be lesser than the amount of energy that is returned. Although renewables were able to produce energy greater than the amount of energy they have used, issues like variability, intermittency, lack of technology for efficient energy storage, high cost of raw materials etc., deterred the usage of the renewables in main stream energy production.

However, recent technological advancements, especially in solar energy sector such as the usage of new materials, reducing the influence of raw material price of absorbent layer on the overall cost of the cell and also recent reduction in prices of raw materials have resulted in achievement of near grid parity. Some projections show that even grid parity is achievable in near future [6], which implies that renewables especially solar energy can be harvested on a large scale so as to give the major chunk of electricity used.

1.2 SOLAR ENERGY

Solar cells, at present, are one of the most extensive forms of renewable energy in the civilian and military domains. Several solar projects have been commissioned by the Marine Corps for stationary units, mobile units, and patrolling Marines. As technology advances, these systems have become smaller and more efficient. However, cost has not been shown to decrease proportional to technological advancement. In the face of decreasing budgets and cuts to military spending, the need for efficient and inexpensive solar cells is desired. Thin film solar cells present an attractive option due to their lightweight and flexible nature. Leading the thin film market are cells constructed from copper indium gallium di-selenide (CIGS), a compound quaternary semiconductor alloy. The robust material properties of CIGS cells present many attractive features for both military and consumer applications, such as mechanical flexibility and durability. One of the most desirable traits is the low cost of manufacturing CIGS cells. Although CIGS cells currently lack the efficiency of silicon (Si) based cells or more advanced multi-junction cells, continued research shows promise in closing this gap while still retaining all the desired qualities of CIGS. Optimization of the design parameters of CIGS structures is necessary to fully maximize the capabilities of cells which will be used in future systems.

1.3 OBJECTIVE

Based on the background summarized in the forgoing sections, the present research aims at covering the following objectives to improve the efficiency of thin film solar cell. The objectives are-

- To find optimal point of different parameters
- To determine the value of intermediate band gap energy for CIGS solar cell
- To find out the effect of different buffer layer in the efficiency of solar cell
- To find the optimum thickness of buffer layer in the efficiency of solar cell
- To know the effect of absorber layer thickness in CIGS solar cell

1.4 STRUCTURE OF THE THESIS

This thesis is arranged into four chapters. The theoretical background into the physics of solar cells and the solar spectrum is given in Chapter-2. An in depth analysis of CIGS cells is given in Chapter-2. An introduction to SCAPS and the results of simulation is given in Chapter-3. The conclusion with recommendations for future work is given in Chapter 4.

Chapter-2

THEORETICAL BACKGROUND

2.1 Solar cell history

The history of solar cells is extensive, with countless discoveries leading to the advances in solar cell technology. Below are a few of the accomplishments.

The introduction of solar cell technology begins as early as 1839. French physicist, Antione-Cesar Becquerel, observed the photovoltaic effect while experimenting with a solid electrode in an electrolyte solution. He noticed a voltage generated when light fell upon the electrode.

Nearly 50 years later, Charles Fritts, an American inventor, spent endless hours creating the first true solar cell. In an attempt to prove to his friends that sunlight could be converted into electricity. The first true solar cells, using junctions, were formed by coating the selenium semiconductor with an extremely thin, nearly transparent layer of gold. As a result of the properties of selenium, Fritt's cells had a conversion efficiency of only about 1%. The high cost of materials, in addition to its inefficiency prevented the use of such cells for energy supply.

The Fritts' first solar cell is shown below. Which had been purchased at an auction by an auctions dealer, only to be forgotten in a box for 60 years. Too much suprise the device still works after being re-discovered

In 1905, Albert Einstein published his paper on the photoelectric effect. Einstein described light as a collection of discrete quanta (photons) rather than continuous waves. He theorized that a photon above a threshold frequency had enough energy to eject a single electron, bonded to an atom (the photoelectric effect). Einstein's interpretation of the photoelectric effect won him the Nobel Prize in Physics in 1921.

In 1953 Photovoltaic technology is born in the United States. Gerald Pearson, an empirical physicist, unintentionally developed a substantially more efficient photovoltaic cell from silicon as opposed to the traditional selenium. The following year, Gerald Pearson, Daryl Chapin, and Calvin Fuller developed the first silicon photovoltaic cell at Bell Laboratories. The silicon solar cell developed

had a 4% efficiency and later achieved 11% efficiency. The device was the first solar cell capable of converting enough of the sun's energy into power to run electrical equipment.

The technical progress of silicon solar cells continued at a fast pace. However, initially the only demand for silicon solar cells was for radio and toy manufacturers to power small devices. As progression of the solar cell continued during the 1950s. NASA began to investigate solar cells to power its ambitious space ventures. In the late 1950s the Vanguard I space satellite used a solar cell to power its radios.

Since the beginning of applications for solar cells, its potential continues to grow rapidly. With modern dependence of fossil fuels, advancements in the efficiency and capabilities of solar power is becoming an increasingly viable power source [8].

2.2 Solar cell physics

Solar cells generate electricity when illuminated; these can be considered as basic building blocks of a photovoltaic system. In general, it can be assumed that a solar cell is equivalent to a two terminal device which acts as a normal diode in a dark environment and as a current source when illuminated.
Normally a voltage of 0.1V is developed by a typical Solar Cell when illuminated, and the short circuit current developed is around 10mA/cm2. As the voltage is really small, large numbers of cells usually in count of 36 or 72 are connected in series on the panel to get a standard voltage of around 12V.

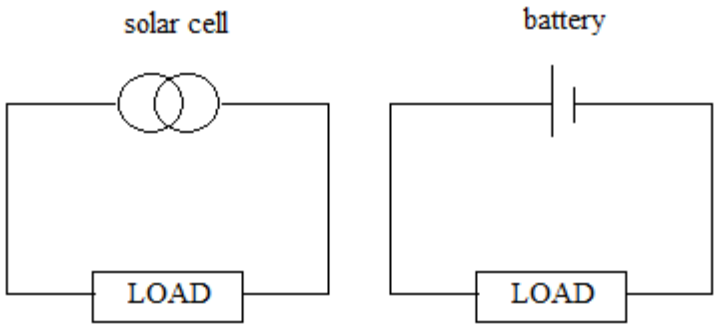

Figure: 2-1 Analogy between solar cell and battery.

From above figures it can be observed that, in conductors, the energy band is continuous and thus the charge carriers do not require any energy to flow from one band to other. Whereas, in the Semiconductors the valence band is full, and there exists a clear band gap between valance band and next energy band i.e., conduction band. The electrons in VB (valance band) are tightly bonded, and energy equivalent to band gap is required to excite those e-`s from VB to CB (conduction band). So the semiconductors at normal conditions act as insulators. The band gap of semiconductor is around 0.5eV to 3eV.

2.3 Basic operation of Solar Cell

The figure 2-2 shows the Energy band structures of conductors, semiconductors and insulators.

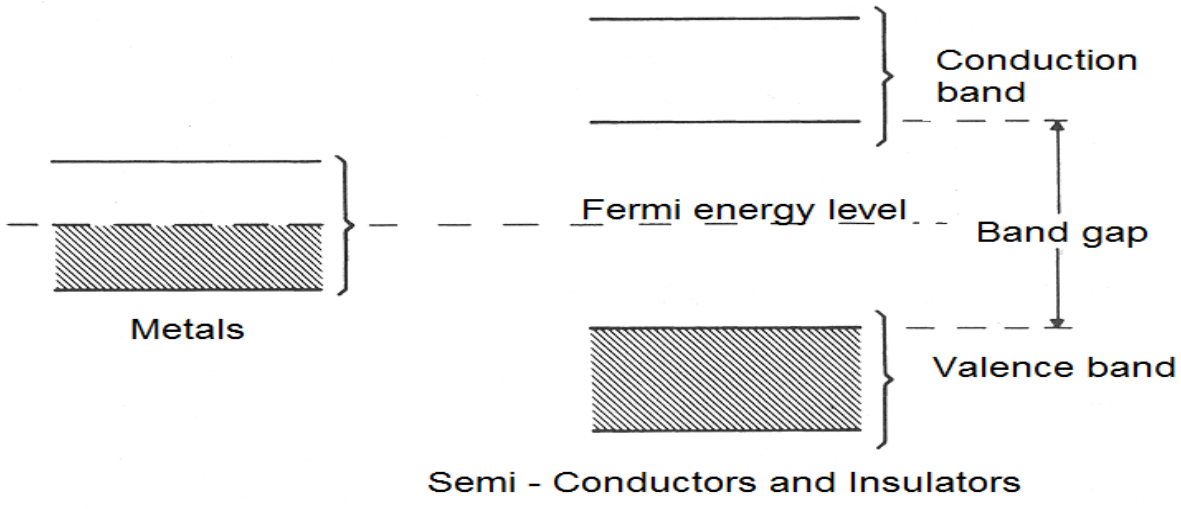

Figure: 2-2 Energy band structures of conductors, semiconductors and insulators.

From above figures it can be observed that, in conductors, the energy band is continuous and thus the charge carriers do not require any energy to flow from one band to other. Whereas, in the Semiconductors the valence band is full, and there exists a clear band gap between valance band and next energy band i.e., conduction band. The electrons in VB (valance band) are tightly bonded, and energy equivalent to band gap is required to excite those e-`s from VB to CB (conduction band). So the semiconductors at normal conditions act as insulators. The band gap of semiconductor is around 0.5eV to 3eV.

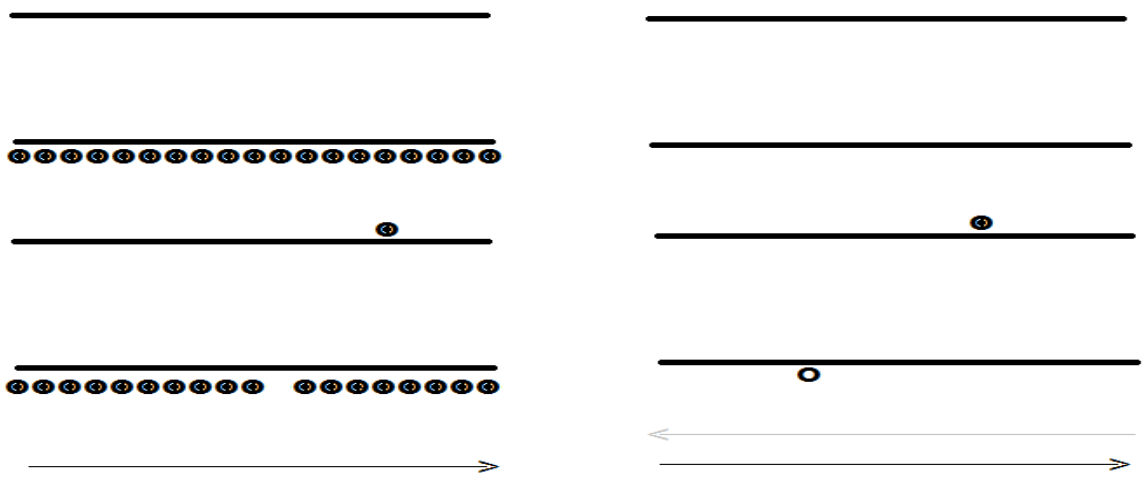

Figure: 2-3 Movement of electrons and holes in p-n junction solar cell [9]

When the electrons in the valance band are exposed to energy greater than their band gap, electron frees itself from the lattice and moves to conduction band leaving a hole in valance band, thus resulting in a free electron hole pair. This electron hole pair is available to conduct electricity. If the exciting energy is provided by an incoming photon, then the entire process is called photo conductivity. Different materials exhibit different levels of photo-conductivity. The photo-conductivity property of material depends on the energy band gap of the material and electron hole recombination's occurring in it. If the material has high energy band gap then high energy photons are needed to move the electrons from Valance band.

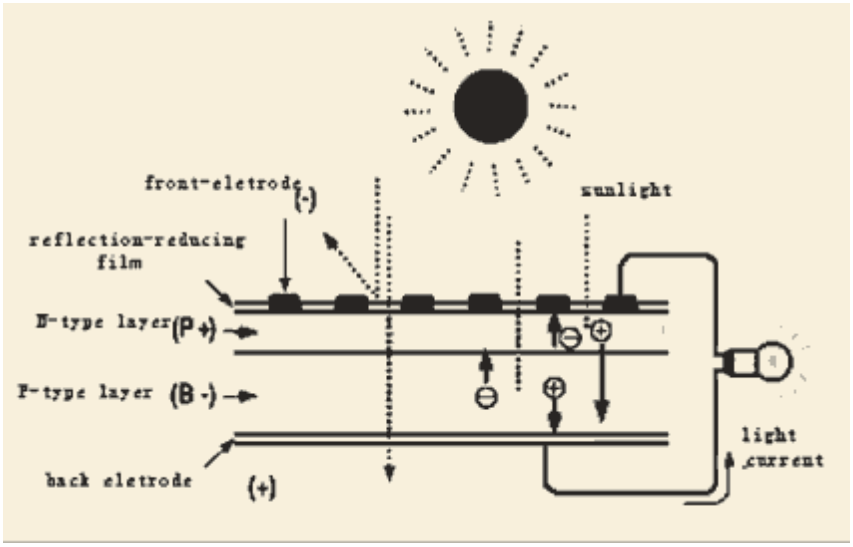

Figure: 2-4 Generation and movement of charge carriers in p-n junction solar cell [9]

A p-n homo junction solar cell has a single material which is n-type doped on the one side and p-type doped on the other. In whole, the cell can be described to be electrically neutral, and the junction region consists of two depletion regions, one with electrons and other with holes on either side.

As shown in the above figure: 2-3 the p-n homo junction, solar cell when illuminated produces an electron hole pair due to the photon absorption and movement of electron from the valence band to the conduction band.

The band structures of p-n junction under equilibrium and illuminated conditions are shown in Fig. 2-5. As shown in figure, the incoming photon excites the electron resulting in an electron hole pair. These charge carriers were used for conduction [10]

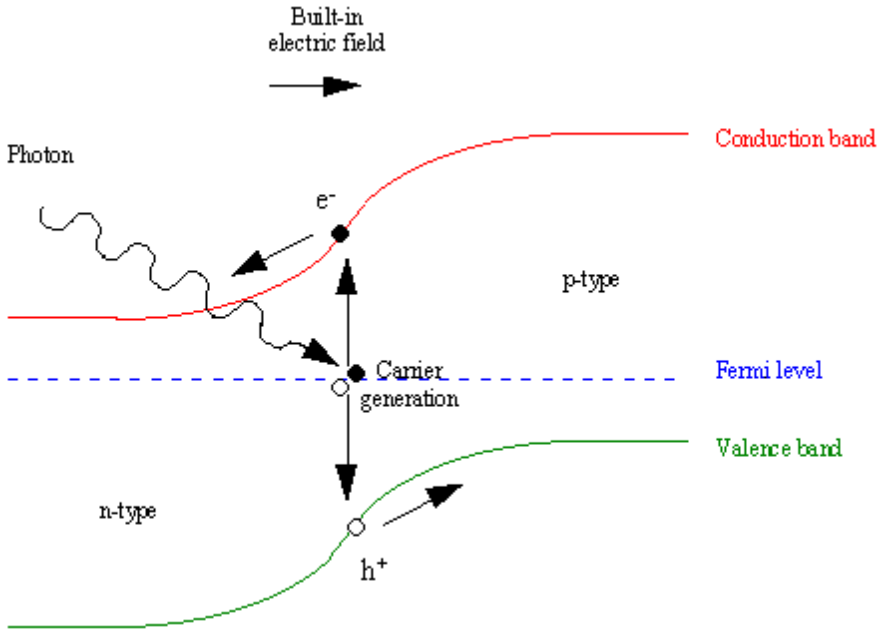

Figure: 2-5 Band structure of PN junction solar cell [11]

2.4 Solar Non-Idealities

There are several factors that can degrade the performance of solar cells. Primary losses can include reflection of photons off the surface of the cell, shading from the top grid, photons that are below band gap, and recombination losses. Typical losses in solar cells are depicted in Figure: 2-6.

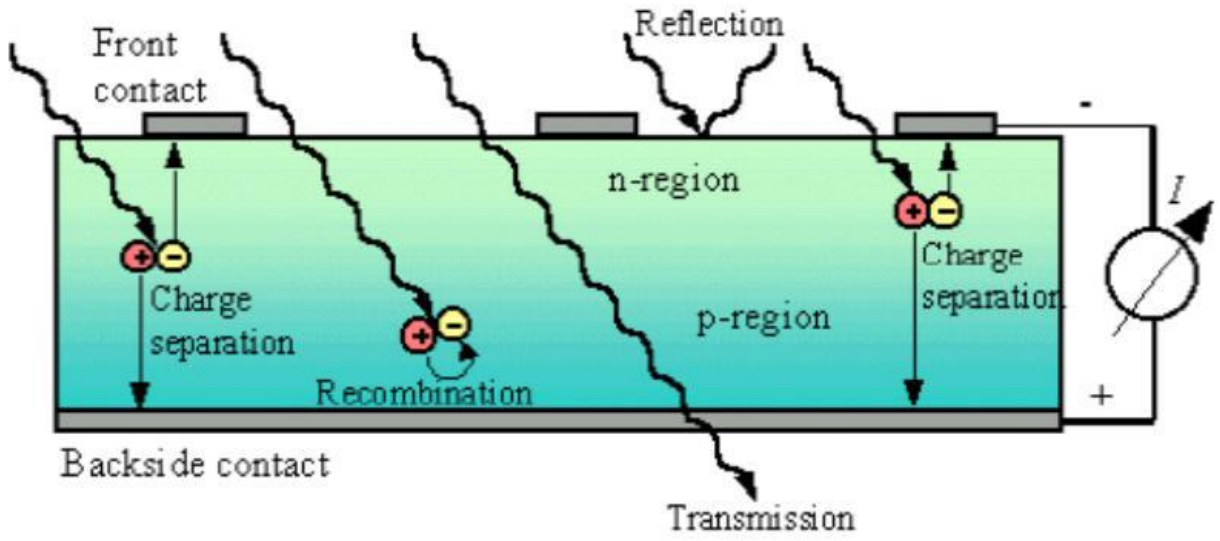

Figure: 2-6 Photoelectric affect in solar cells [12]

An in-depth explanation of solar cell losses is found in [20]. Optimizing solar cell efficiencies by targeting the correct band gap and optimum cell thickness for absorptions is investigated.

2.5 SOLAR SPECTRA IRRADIATION ON EARTH

The sun produces light at various intensities throughout the wavelength spectrum. These intensities are closely mimicked by a 6000 K black body radiation. As the light travels through space, its intensity decreases by a rate of 1/d2 where d is the distance from the sun [13]. The standard for measuring light intensity on earth is to describe by how many atmospheres the light has passed through. The intensity spectrum for satellites in space is labeled as AM0, since the light has not passed through any of the earth's atmosphere. At sea level, near the equator, at noon on a cloudless day, the spectrum is labeled as AM1, since light has passed through one standard atmosphere. As not all solar cells are utilized on the equator at noon, the industry standard for measuring solar cell is AM1.5, or one and a half atmospheres. Intensity losses in this spectrum are due to photon absorption by particulates in the atmosphere. The most notable of these are ozone (O3), water (H2O), and carbon dioxide (CO2) [16]. These absorption losses are represented by deep troughs as seen in Figure: 2-6.

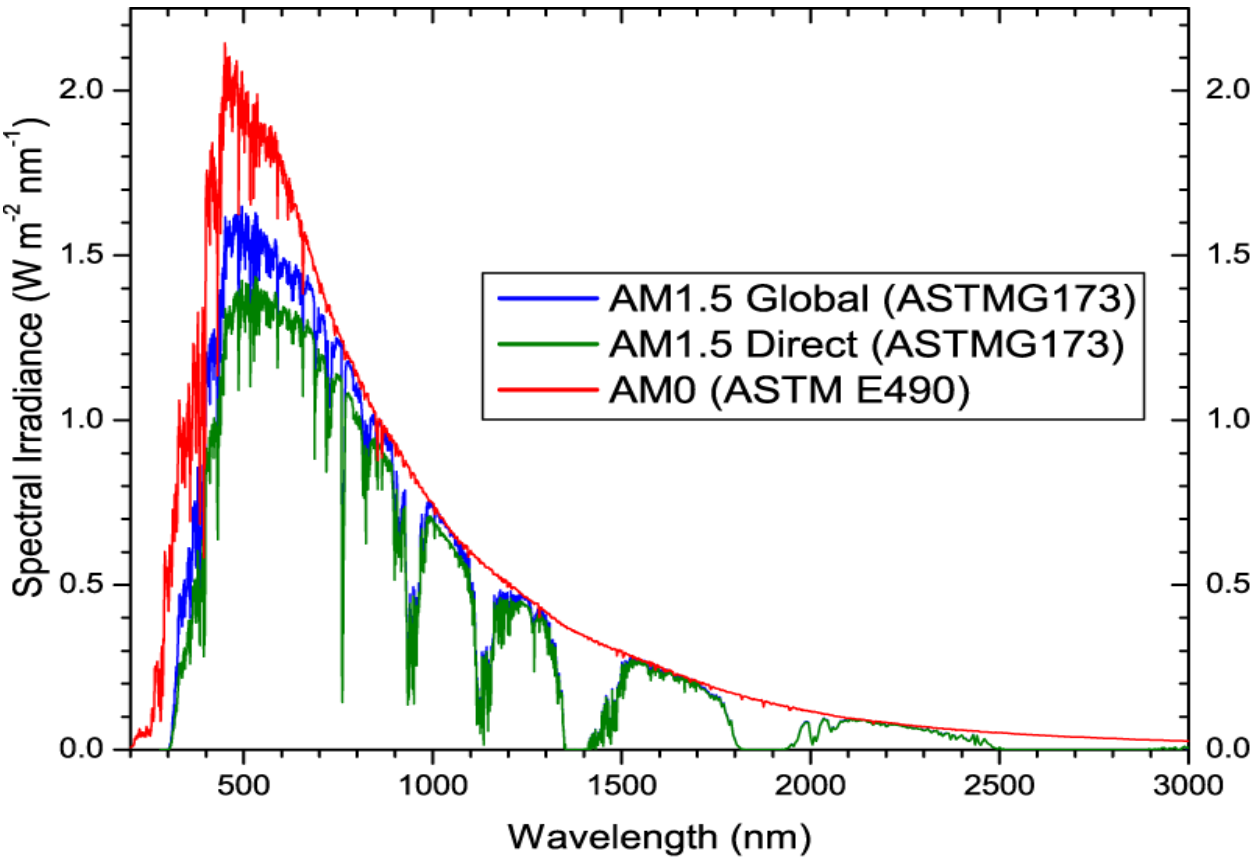

Figure: 2-7 Solar spectral irradiance versus wavelength for differing standards [12]

While absorption losses are represented as deep troughs in the spectrum, this does not account for the general loss of intensity. General intensity loss is due to reflection and scattering of photons by air molecules and dust particles in the atmosphere [13].

As stated earlier, the industry standard is AM1.5. This spectrum gives a relative baseline for which all solar cells are tested against. AM1.5 is not representative of the solar spectrum at all locations on the Earth; it is merely used for standardization. Besides atmospheric effects, spectrum intensity is most influenced by altitude, humidity, and latitude. Solar cells at higher altitudes are exposed to more intense radiation than those at sea level. An arid climate has less photon absorption by water molecules than a humid climate. Solar cells used near the equator have more direct sunlight than a cell used at higher latitudes with glancing rays. All of these effects can vary the solar spectrum intensity and change the performance of solar cells. By tuning the band gap of CIGS, we can optimize cells for a particular region or climate. A cell that is used in a high altitude desert might have a different optimum band gap than one used at sea level in 100% humidity. By using a cell with an optimized band gap, average power output can be increased without significant changes in the manufacturing process.

2.6 Solar Cell Types

Solar cells can be categorized into three generations based on the material used to manufacture them.

2.6.1 First Generation Solar Cell—Wafer Based

As it is already mentioned, the first generation solar cells are produced on silicon wafers. It is the oldest and the most popular technology due to high power efficiencies. The silicon wafer based technology is further categorized into two subgroups named as

- Single/ Mono-crystalline silicon solar cell.
- Poly/Multi-crystalline silicon solar cell.

2.6.1.1 Single/Mono-Crystalline Silicon Solar Cell

Mono crystalline solar cell, as the name indicates, is manufactured from single crystals of silicon by a process called Czochralski process [14]. During the manufacturing process, Si crystals are sliced from the big sized ingots. These large single crystal productions require precise processing as the process of “recrystallizing” the cell is more expensive and multi process. The efficiency of mono-crystalline single-crystalline silicon solar cells lies between 17% - 18% [15].

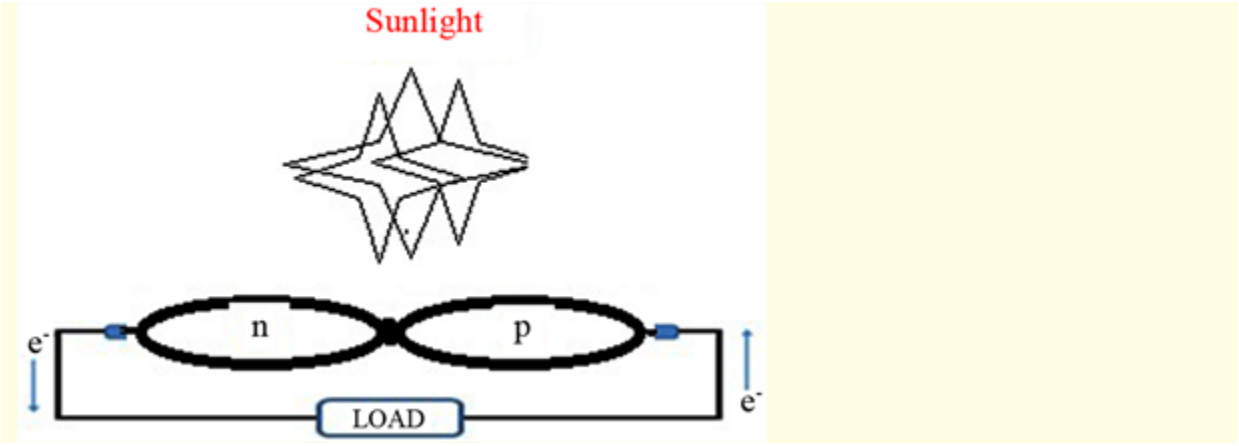

Figure: 2-8 The semiconductor p-n junction solar cell under load.

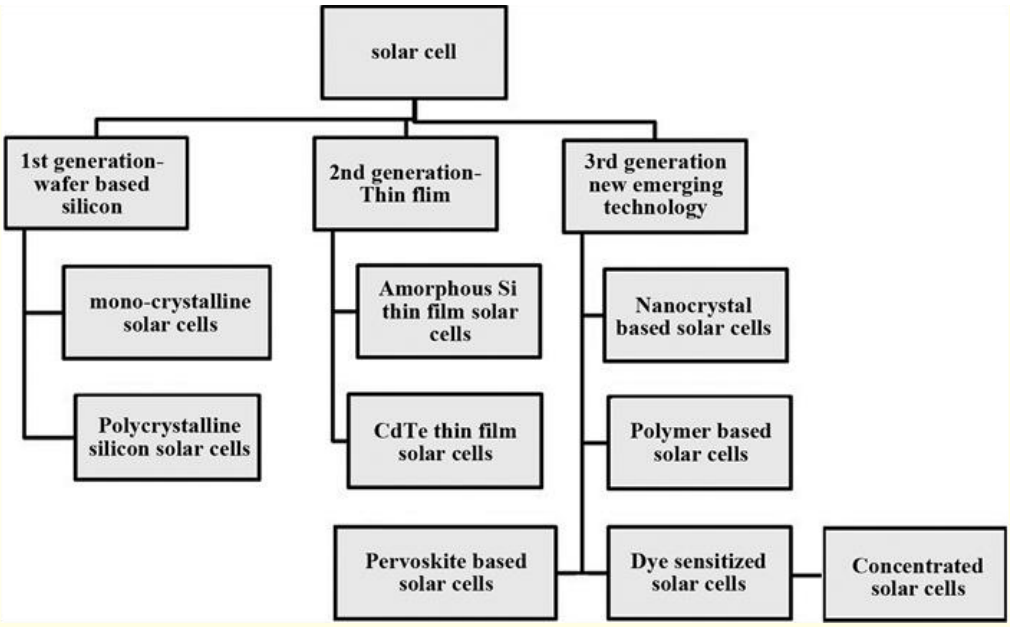

Figure: 2-9 Various types of solar cell technologies and current trends of development.

2.6.1.2 Polycrystalline Silicon Solar Cell (Poly-Si or Mc-Si)

Polycrystalline PV modules are generally composed of a number of different crystals, coupled to one another in a single cell. The processing of polycrystalline Si solar cells is more economical, which are produced by cooling a graphite mold filled containing molten silicon. Polycrystalline Si solar cells are currently the most popular solar cells. They are believed to occupy most up to 48% of the solar cell production worldwide during 2008 [16] During solidification of the molten silicon, various crystal structures are formed. Though they are slightly cheaper to fabricate compared to monocrystalline silicon solar panels, yet are less efficient ~12% - 14% [17]

2.6.2 Second Generation Solar Cells—Thin Film Solar Cells

Most of the thin film solar cells and a-Si are second generation solar cells, and are more economical as compared to the first generation silicon wafer solar cells. Silicon-wafer cells have light absorbing layers up to 350 µm thick, while thin-film solar cells have a very thin light absorbing layers, generally of the order of 1 µm thickness [18]. Thin film solar cells are classified as

- a-Si.
- CdTe.
- CIGS (copper indium gallium di-selenide).

2.6.2.1 Amorphous Silicon Thin Film (a-Si) Solar Cell

Amorphous Si (a-Si) PV modules are the primitive solar cells that are first to be manufactured industrially. Amorphous (a-Si) solar cells can be manufactured at a low processing temperature, thereby permitting the use of various low cost, polymer and other flexible substrates. These substrates require a smaller amount of energy for processing [19]. Therefore, a-Si amorphous solar cell is comparatively cheaper and widely available. The “amorphous” word with respect to solar cell means that the comprising silicon material of the cell lacks a definite arrangement of atoms in the lattice, non-crystalline structure, or not highly structured. These are fabricated by coating the doped silicon material to the backside of the substrate/glass plate. These solar cells generally are dark brown in color on the reflecting side while silverish on the conducting side [20].

The main issue of a-Si solar cell is the poor and almost unstable efficiency. The cell efficiency automatically falls at PV module level. Currently, the efficiencies of commercial PV modules vary in the range of 4% - 8%. They can be easily operated at elevated temperatures, and are suitable for the changing climatic conditions where sun shines for few hours [21] .

2.6.2.2 Cadmium Telluride (CdTe) Thin Film Solar Cell

Among thin-film solar cells, cadmium telluride (CdTe) is one of the leading candidate for the development of cheaper, economically viable photovoltaic (PV) devices, and it is also the first PV technology at a low cost. CdTe has a band gap of ~1.5 eV as well as high optical absorption coefficient and chemical stability. These properties make CdTe most attractive material for designing of thin-film solar cells.

CdTe is an excellent direct band gap crystalline compound semiconductor which makes the absorption of light easier and improves the efficiency. It is generally constructed by sandwiching between cadmium sulfide layers to form a p-n junction diode. The manufacturing process involves three steps: Firstly, the CdTe based solar cells are synthesized from polycrystalline materials and glass is chosen a substrate. Second process involves deposition, i.e., the multiple layers of CdTe solar cells are coatedon to substrate using different economical methods. It is already mentioned that CdTe has a direct optimum band gap (~1.45 eV) with high absorption coefficient over 5×10^{15}/cm [22] . Therefore, its efficiency usually operates in the range 9% - 11% [23].CdTe solar cells can be made on polymer substrates and flexible. However, there are various environmental issues with cadmium component of solar cell. Cadmium is regarded as a heavy metal and potential toxic agent that can accumulate in human bodies, animals and plants. The disposal of the toxic Cd based materials as well as their recycling can be

highly expensive and damaging too to our environment and society. Therefore, a limited supply of cadmium and environmental hazard associated with its use are the main issues with this CdTe technology.

2.6.2.3 Copper Indium Gallium Di-Selenide (CIGS) Solar Cells

CIGS is a quaternary compound semiconductor comprising of the four elements, namely: Copper, Indium, Gallium and Selenium. CIGS are also direct band gap type semiconductors. Compared to the CdTe thin film solar cell, CIGS hold a higher efficiency ~10% - 12%. Due to their significantly high efficiency and economy, CIGS based solar cell technology forms one of the most likely thin film technologies. The processing of CIGS are done by the following techniques: sputtering, evaporation, electrochemical coating technique, printing and electron beam deposition. In addition, the sputtering can be a two or multi-step process involving with deposition and subsequent interaction with selenium later, or can be a one-step reactive process. However, evaporation is similar to the sputtering in the sense that it can be used in a single step, two-step or multiple processing steps. The substrates for CIGS material can be chosen from glass plate, polymers substrates, steel, aluminum etc. The advantages of CIGS thin film solar cells include its prolonged life without a considerable degradation. These properties of CIGS indicate an easy solution to enhance the efficiency [24]

2.6.3 Third Generation Solar Cells

Third generation cells are the new promising technologies but are not commercially investigated in detail. Most of the developed 3rd generation solar cell types are:

1) Nano crystal based solar cells.
2) Polymer based solar cells.
3) Dye sensitized solar cells.
4) Concentrated solar cells.

2.6.3.1 Nano Crystal Based Solar Cells

Nanocrystal based solar cells are generally also known as Quantum dots (QD) solar cells. These solar cells are composed of a semiconductor, generally from transition metal groups which are in the size of nanocrystal range made of semiconducting materials. QD is just a name of the crystal size ranging typically within a few nanometers in size, for example, materials like porous Si or porous TiO_2, which are frequently used in QD. With the advance of nanotechnology, these nanocrystals of semiconducting material are targeted to replace the semiconducting material in bulk state such as Si, CdTe or CIGS. This idea of the QD based solar cell with a theoretical formulation were employed for the design of a p-i-n solar cell over the self-organized in As/GaAs system [25]. Generally, the nanocrystals are mixed into a bath and coated onto the Si substrate. These crystals rotate very fast and flow away due to the centrifugal force. In conventional compound semiconductor solar cells, generally a photon will excite an electron there by creating one electron-hole pair [26]. However, when a photon strikes a QD made of the similar semiconductor material, numerous electron-hole pairs can be formed, usually 2 or 3, also 7 has been observed in few cases.

Table 2-1. A comparison of various types of solar cells [16] [17].

Table 1. A comparison of various types of solar cells [16] [17].

Cell type	Crystalline silicon		Thin Film			Third Generation				Perovskites
	Monocrystalline	Polycrystalline	CdTe	CIGS	Amorphous Silicon	Nanocrystal	Dye Sensitized	Polymer	Concentrated	
Efficiency	14% - 17.5%	12% - 14%	9% - 11%	10% - 12%	4% - 8%	7% - 8%	≈10%	≈3% - 10%	≈40%	31%
High temperature performance	Not good at high temperatures	Not good at high temperatures	Good in cool as well as high temperature conditions	Good in cool as well as high temperature conditions	Good in cool as well as high temperature conditions	Excellent thermal stability	Not good in high temperature conditions	Not good in high temperature conditions	Excellent thermal stability	Excellent thermal stability
Size	Significantly less volume to produce the same amount of power	Significantly less volume to produce the same amount of power	Offering a wide range of product design from flexible, light durable	Offering a wide range of product design from flexible, light durable	Offering a wide range of product design from flexible, light durable	Offering a wide range of product design from flexible, light durable	Offering a wide range of product design from flexible, light durable	Offering a wide range of product design from flexible, light durable	Offering a specialized range of product design	Offering a wide range of product design from flexible, light durable
Cost	Two times more expensive compared to thin-film.	Two times more expensive compared to thin-film.	50 percent less expensive than conventional silicon cells	50 percent less expensive than conventional silicon cells	50 percent less expensive than conventional silicon cells	50 percent less expensive than conventional silicon cells	50 percent less expensive than conventional silicon cells	50 percent less expensive than conventional silicon cells	50 percent less expensive than conventional silicon cells	50 percent less Expensive than conventional silicon cells
Additional detail	Oldest PV technology	Economical choice	Toxic due to Cd	Some CIGS have impressive 20% efficiency	Needs long installation time and large space	Needs short installation time and large space	Needs short installation time and large space	Needs short installation time and small space	Needs long installation time and large space	Latest technology. Needs short installation time and minimum space

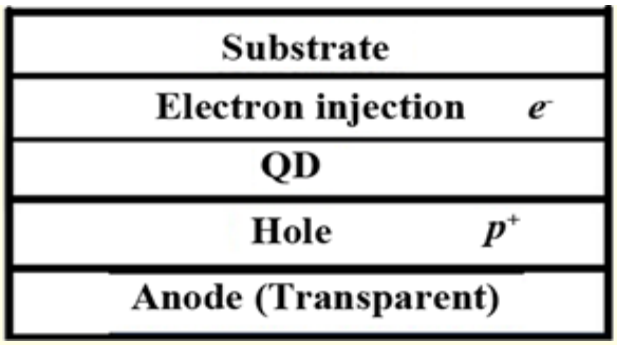

Figure: 2-10 A schematic of Quantum dot (QD) layer.

2.6.3.2 Polymer Solar Cells

Polymer solar cells (PSC) are generally flexible solar cells due to the polymer substrate. The first PSC were invented by the research group of Tang et al. at Kodak Research Lab. [27]. A PSC is composed of a serially connected thin functional layers coated on a polymer foil or ribbon. It works usually as a combination of donor (polymer) and a acceptor (fullerene). There are various types of materials for the absorption of sunlight, including organic material like a conjugate/conducting polyme . In 2000, Heeger, MacDiarmid, and Shirakawa fetched the Nobel Prize in Chemistry for the discovering a new category of polymer materials known as conducting polymers. The PSC and other organic solar cells operate on same principle known as the photovoltaic effect, i.e., where the transformation of the energy occurs in the form of electromagnetic radiations into electrical current. Yu et al. mixedpoly [2-methoxy-5-(2'-ethylhexyloxy)-p-phenylene vinylene] (PPV), C60 and its other derivatives to develop the first polymer solar cell and obtained a high power conversion efficiency. This process triggered the development of a new age in the polymer materials for capturing the solar power. After significantly optimizing the parameters, researchers achieved efficiency over 3.0% for PPV type PSCs [28]. These unique properties of PSCs opened a new gateway for new applications in the formation of stretchable solar devices including textiles and fabrics [39]. A modern recycling concept known as polarizing organic photovoltaics (ZOPVs) was also developed for increasing the function of liquid crystal displays utilizing the same polarizer, a photovoltaic device and proper light conditions/solar panel.

2.6.3.3 Dye Sensitized Solar Cells (DSSC)

Recent research has been focused on improving solar efficiency by molecular manipulation, use of nanotechnology for harvesting light energy. The first DSSC solar cell was introduced by Michel Gratzel in Swiss federal institute of technology [29]. DSSCs based solar cells generally employ dye molecules between the different electrodes. The DSSC device consists of four components: semiconductor electrode (n-type TiO_2 and p-type NiO), a dye sensitizer, redox mediator, and a counter electrode (carbon or Pt). The DSSCs attractive due to the simple

conventional processing methods like printing techniques, are highly flexible, transparent and low cost as well. The novelty in the DSSC solar cells arise due to the photosensitization of nano grained TiO2 coatings coupled with the visible optically active dyes, thus increasing the efficiencies greater than 10% [30]. However, there are certain challenges like degradation of dye molecules and hence stability issues. This is due to poor optical absorption of sensitizers which results in poor conversion efficiency. The dye molecules generally degrade after exposure to ultraviolet and infrared radiations leading to a decrease in the lifetime and stability of the cells. Moreover, coating with a barrier layer may also increase the manufacturing more expensive and lower the efficiency.

2.6.3.4 Concentrated Solar Cell

Concentrating photovoltaic (CPV) has been established since the 1970s [31]. It is the newest technology in the solar cell research and development. The main principle of concentrated cells is to collect a large amount of solar energy onto a tiny region over the PV solar cell, as shown in Figure 5. The principle of this technology is based on optics, by using large mirrors and lens arrangement to focus sunlight rays onto a small region on the solar cell. The converging of the sunlight radiations thus produces a large amount of heat energy. This heat energy is further driven by a heat engine controlled by a power generator with integrated. CPVs have shown their promising nature in solar world. It ca n be classified into low, medium, and high concentrated solar cells depending on the power of the lens systems. Concentrating photovoltaic technology have the following merits, such as solar cell efficiencies >40%, absence of any moving parts, no thermal mass, speedy response time and can be scalable to a range of sizes.

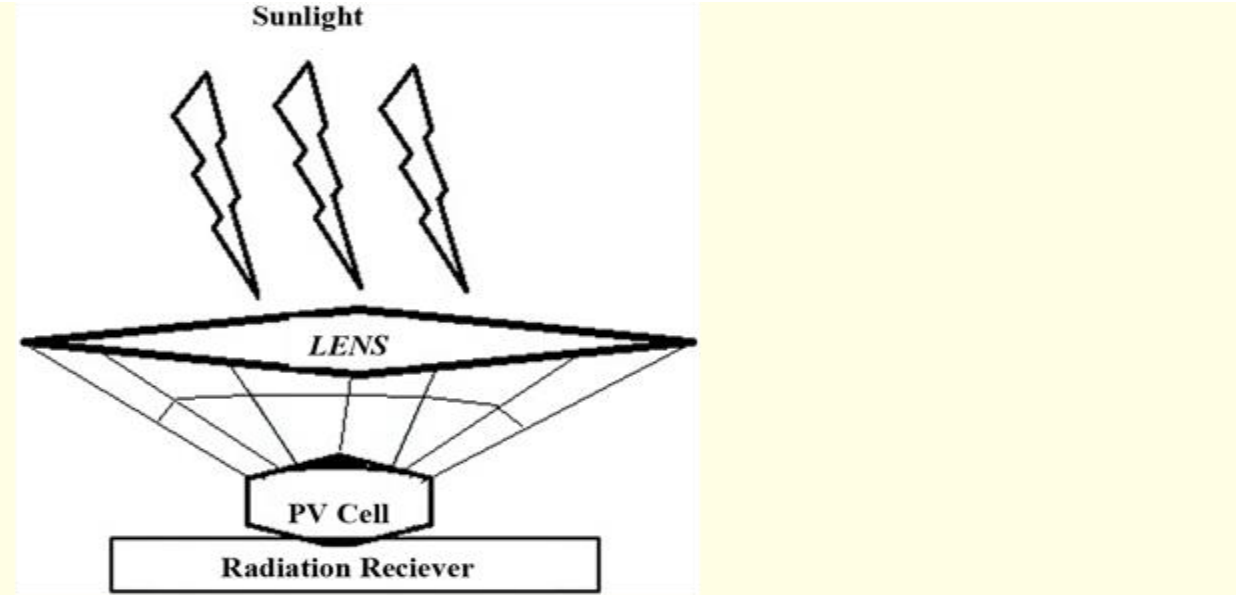

Figure: 2-11 Schematic of concentrated solar cell [31].

2.6.3.5 Perovskite Based Solar Cell

Perovskites are a class of compounds defined by the formula ABX_3 where X represents a halogen such as I^-, Br^-, Cl^-. and A and B are cations of different size. Perovskite solar cells are recent discovery among the solar cell research community and possess several advantages over conventional silicon and thin film based solar cells. Conventional Si based solar cells need expensive, multiple processing steps and require high temperatures (>1000˚C) and vacuums facilities [34]. The perovskites based solar cells can have efficiency up to 31% [32]. It can be predicted that these perovskites may also play an important role in next-generation electric automobiles batteries, according to an interesting investigation recently performed by Volkswagen. However, current issues with perovskite solar cells are their stability and durability. The material degrades over time, and hence a drop in overall efficiency. Therefore more research is needed to bring these cells into the market place.

2.7 *CIGS SOLAR CELLS*

BASIC STRUCTURE

Modern commercially produced CIGS cells consist of five layers, each with their own unique parameters and function. The typical design of a CIGS cell is shown in Figure 3-1.

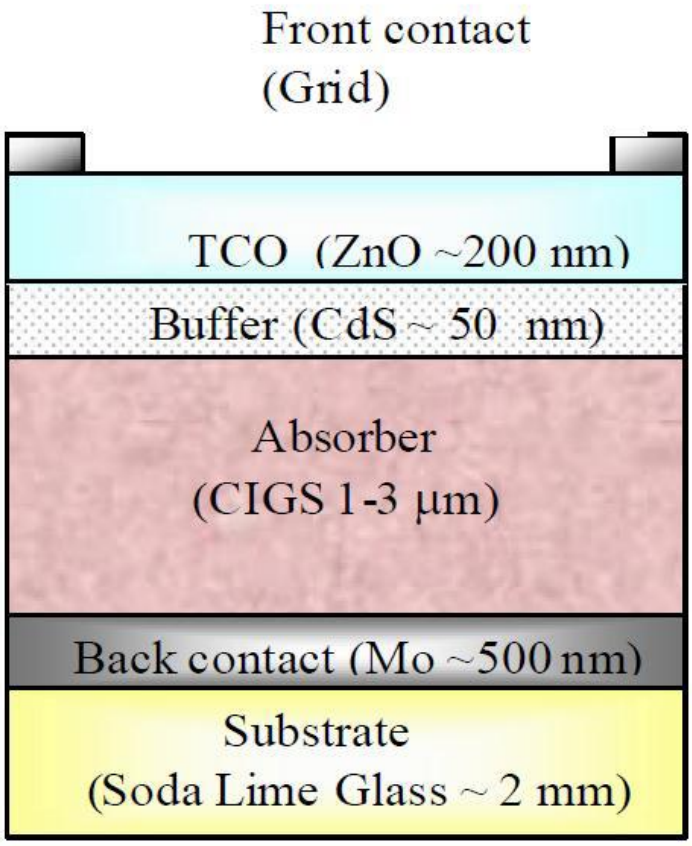

Figure: 3-1 CIGS basic structure

The cells are "grown" beginning with the substrate. Each additional layer is then deposited via various commercially available means. The numerous manufacturing techniques for fabricating CIGS cells are not investigated in this thesis but some of their limitations are taken into account.

2.7.1. Substrate

The substrate is the starting point for the manufacture of CIGS and is what determines whether the solar cell is flexible or rigid. Glass is the most common substrate used in production solar

cells due to its low cost and ability to resist corrosion. Soda lime glass (SLG) is often used in manufacturing for its contribution to increasing performance properties. It has been shown that during the manufacturing process, sodium particles from the substrate diffuse into the back contact layer and increase efficiency. While this phenomenon is still being investigated, it has been proven that, all things being equal, cells manufactured on SLG have higher efficiency than other commonly used substrates. The use of SLG as a substrate offers many benefits to CIGS solar cells but has one major drawback. Any glass substrate negates the ability of thin film cells to be light weight and flexible. Metals such as stainless steel or aluminum offer a suitable substrate that allow the solar cell to remain lightweight and flexible. Thin plastics and polymers can also be used as a viable replacement to SLG. As stated in [33], "Typical thickness of metal, polymer, or ceramic substrate materials is generally between 25 and 400 um, about one or two orders of magnitude lower than standard SLG substrates." By using certain metals as substrates, manufactures are able to retain the lightweight and flexible properties that are desired in CIGS cells.

2.7.2 Back Contact

The back contact of a solar cell is placed between the bottom of the absorber layer and the top of the substrate as seen in Figure 17. The back contact layer is designed to collect the carriers as they are produced in the absorber layer. The back contact in solar cells generally consists of a metal with low resistivity and serves as the positive lead or anode of the cell. For CIGS cells, molybdenum (Mo) is used for its compatibility in the manufacturing process [34]

2.7.3. Absorber Layer

The absorber or CIGS layer is where the majority of carrier generation is accomplished. CIGS is an I-III-VI semiconductor known as a chalcopyrite. CIGS is an alloy of the materials CuInSe2 (CIS) and CuGaSe2 (CGS). Both CIS and CGS are direct band gap materials, with band gaps ranging from 1.07 eV to 1.76 eV and a high absorption coefficient. The range of band gap levels covers the infrared and higher energies of the sunlight spectrum. This results in most of the incident sunlight being absorbed close to the p-n hetero-junction formed with the CdS layer. This property is what allows the absorber layer to be manufactured in CIGS cells with thickness orders of magnitude smaller compared to traditional Si cells [34]. By alloying these two compounds, we can vary the band gap of CIGS.

2.7.4. Buffer Layer

The buffer layer is deposited on the absorber layer. CdS is the most widely used buffer layer in the CIGS solar cells. CdS is an n-type semiconductor with a band gap of ~2.4 eV. The buffer layer improves the CIGS solar cells' performance by forming the optimized band alignment between the absorber layer and the window layer. In addition, the buffer layer possesses more advantages to the CIGS solar cells such as the damage prevention of the absorber layer in the sequent sputtering process, the passivation of the absorber surface, the relief of the lattice misfit and so on. Besides CdS, more new buffer layers are in the development process. For example, the new buffer layers include Zn(S,O), ZnMgO, ZnS and In_2S_3. Since the research on the new buffer layers is a hotspot in the development of the CIGS solar cell in recent years, one can search a lot of published papers regarding the new generation Cd-free buffer layers and some of them showed great progress.

2.7.5 Window Layer

A window layer is designed to function in a similar fashion to the back contact. The window layer's purpose is to collect carriers as they are produced and transport them to the load. Since the window layer is on top of the solar cell, it needs to be transparent to the light spectrum that is required for photoelectric effect. To achieve this desired effect, a transparent conducting oxide (TCO) is often used for the window layer. A good TCO has a large enough band gap to allow a majority of photons to reach the absorber layer. It is also critical that the TCO has a low resistivity to reduce recombination losses. In common CIGS cells, zinc oxide (ZnO) is used for the TCO. ZnO has a band gap of 3.3 eV [34]. In this thesis, two layers of ZnO are used. The first layer, placed directly above the buffer layer, is a thin layer of iZnO. This aids in the cell bonding together in the manufacturing process. The second layer is ZnO doped with aluminum to give it low resistivity and increase efficiency.

2.8 Technology of the CIGS solar cells

The term "photo-voltaic" has been in use in English since 1849. A photovoltaic cell (also called a solar cell) is an electrical device that converts the energy of light directly into electricity by the photovoltaic effect [20]. The operation of a solar cell requires three basic attributes. At first, the absorption of light generates either electron-hole pairs or excitons. Afterwards, various types of charge carriers are separated. Finally, those carriers are extracted to an external circuit. Conventionally, photovoltaic materials use inorganic semiconductors. Ideally, the absorber material of an efficient solar cell should be a semiconductor with a bandgap of 1–1.5 eV with a high solar optical absorption (10^4 to 10^5 cm^{-1}) in the wavelength region of 350–1000 nm, a high quantum yield for the excited carriers, a long diffusion length and low recombination velocity [35]

The magnetron sputtering is extensively used to deposit the Mo back contact layer and the ZnO window layer. The CdS buffer layer is usually fabricated by a chemical bath deposition method. Several more methods such as atomic layer deposition and spray ion layer gas reaction technique have been adopted to obtain the new buffer layers. Several techniques were developed to fabricate Cu(In,Ga)Se_2. Among them the co-evaporation method and the two-stage process are two of the most important techniques.

2.9 BENEFITS OF CIGS CELLS MANUFACTURING

The use of CIGS solar cells has the potential to lead the market in thin film solar cells. This is due to the many benefits that CIGS cells offer both to the manufacturer and the consumer. As research continues into improving both the efficiency of the cells and reducing the manufacturing costs, CIGS cells have the potential to gain the majority of the thin film market share [36].

2.9.1 Inexpensive Manufacturing

One of the main benefits of CIGS cells is that they can be commercially manufactured at a fraction of the cost of traditional Si cells. To start with, crystalline Si cells need to be manufactured from extremely pure Si. Once a manufacturer has bulk Si with high enough purity, the material must be heated to extremely high temperatures for it to form in a

crystalline structure. This block of crystalline Si is then cut into wafers that must undergo numerous rounds of etching and doping before a final product is achieved [37]. This process is very time consuming and expensive for the manufacturer. Thin film solar cells, such as CIGS can be produced in a much more efficient manner. The CIGS material can be deposited onto the substrate and back contact by a process called disposition. This essentially sputters the elements onto the substrate at high enough temperature to allow them to adhere. This process does not require the high tolerances of Si cells and is overall a more manufacture-friendly process [32]. In addition to the benefits of disposition, CIGS can be manufactured with a technique call roll-toroll. Roll-to-roll manufacturing is displayed in Figure: 3-2.

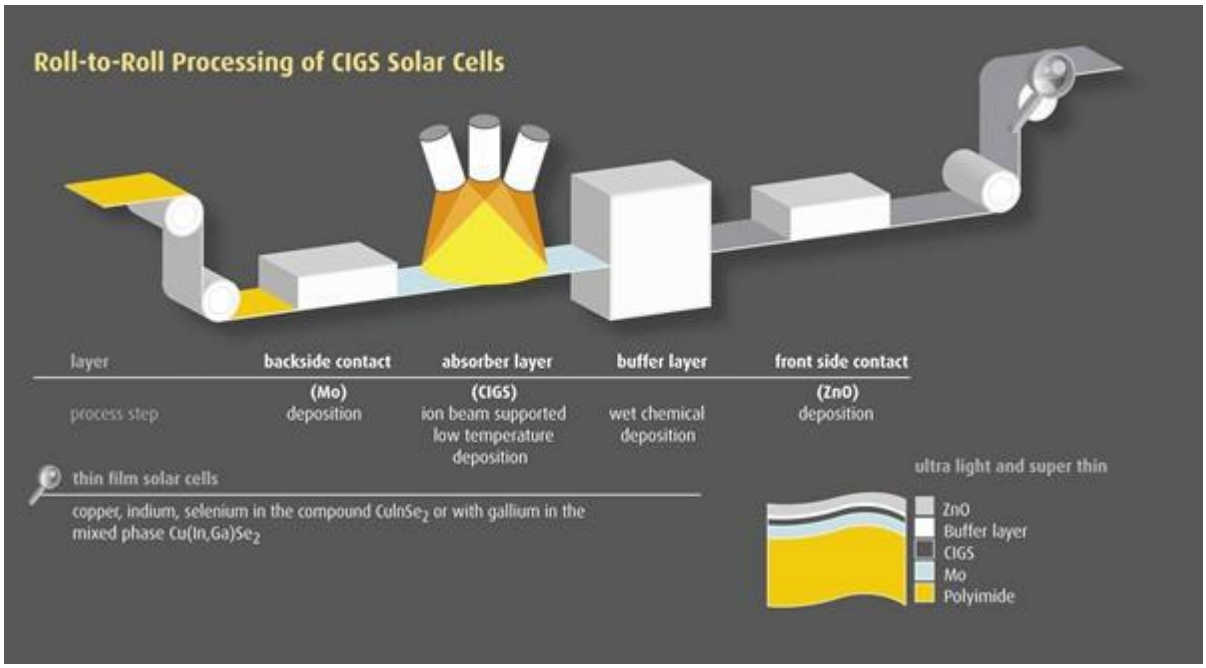

Figure: 3-2 Roll-to-roll processing of CIGS solar cells [38].

2.9.2. Flexible

The flexibility of CIGS cells produced on a thin metal substrate is also a tremendous benefit. This flexibility gives CIGS an advantage over traditional Si cellswith respect to mounting. A standard Si cell has properties consistent with a pane of glass. This makes a Si cell rigid and brittle, restricting the options for implementing solar arrays. The flexible nature of CIGS allows them to be mounted to structures that may notbe perfectly flat. Research has shown the practicality of mounting CIGS cells on dronaircraft, thereby increasing their endurance [39].

2.9.3. Lightweight

A byproduct of being thin and flexible is also being lightweight. Being lightweight has its advantages for people who wish to take their solar cells with them as they travel about. This means that the market for solar cells will be able to increase from the traditional home or industrial power production to more expeditionary ones. CIGS cells could be marketed from campers, backpackers, and general outdoorsmen to beach goers and picnickers. Being lightweight give CIGS cells a portability that remains out of reach for Si based cells.

2.10 CURRENT STATE OF TECHNOLOGY

Research into CIGS cells continues to improve the efficiencies seen in manufactured cells. The National Renewable Energy Laboratory's record efficiencies for numerous solar cell technologies versus the date that the efficiency was recorded is shown in Figure: 3-3.

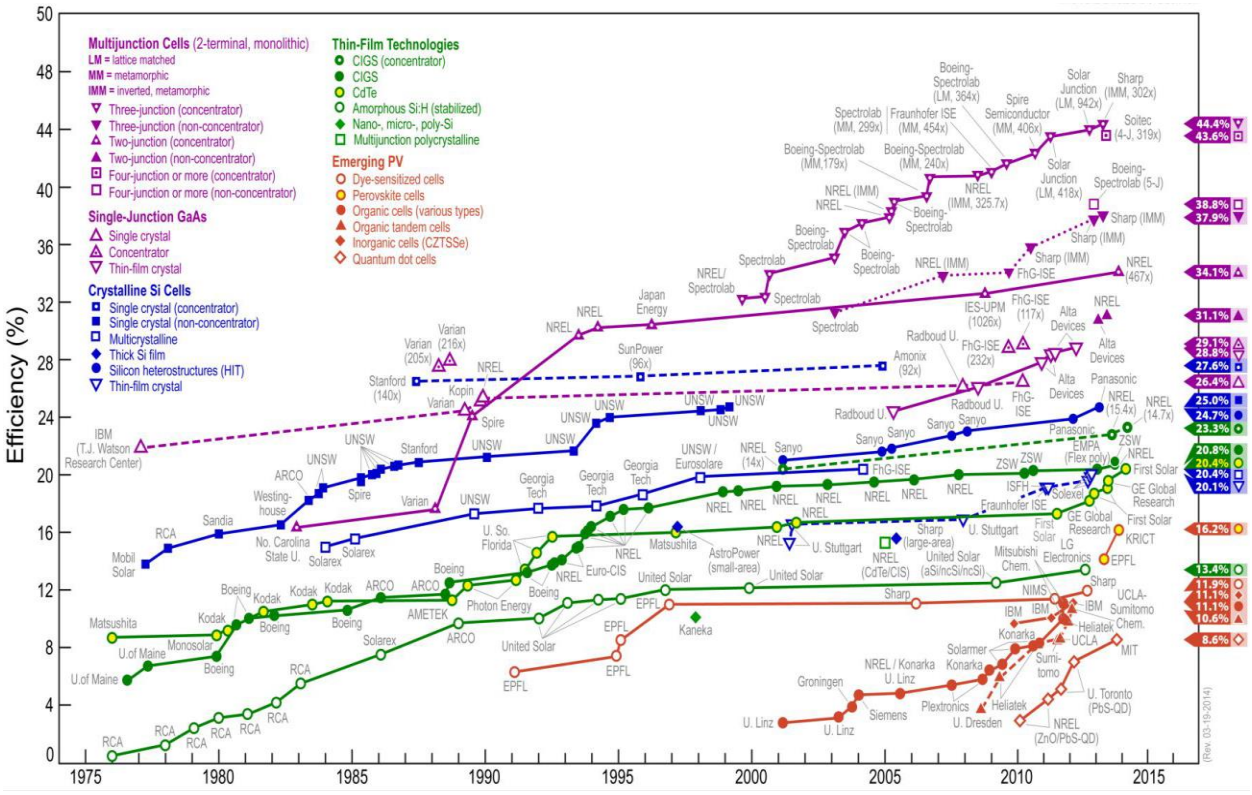

Figure: 3-3 NREL's best research-cell efficiencies versus time [38].

Comparing CIGS cells performance in Figure 21 to other single junction non-concentrated cells, one can see that CIGS cells fall short. The current record for a CIGS cell is 22.8% efficiency, which leads the non-concentrated thin-film technologies. Compare this to a single crystal Si cell with an efficiency of 25.0% or a single crystal gallium arsenide cell with an efficiency of 26.4%, and CIGS cells are simply outpaced [40]. When consumers are looking to power their home with solar cells, efficiency is the driving factor. A cell that is light weight and flexible is of little concern if it has 5% lower efficiency. CIGS cells still have the advantage of being inexpensive. As manufacturers continue to improve the efficiency, CIGS will gain a larger foot hold on the market. While the industry standard is to measure cell efficiency against an irradiance of AM1.5, CIGS ability to have a variable band gap may give users in unique climates higher usable power than similar single junction cells. All these benefits point to an increase in CIGS demand with manufactures finding ways to increase efficiency and decrease production costs.

2.11 CONCLUSION

An in-depth look at CIGS solar cells was given in this chapter. The basic layers were discussed as well as the numerous benefits that CIGS possess over comparable cells. An explanation into how CIGS cells can be manufactured with various band gaps was given as well as the benefit that this offers to consumers. Finally, the current state of CIGS was discussed and compared to other solar cells that are on the market today.

Chapter-3

RESULTS AND DISCUSSIONS

3.1 SCAPS BASIC

SCAPS is a one dimensional solar cell simulation program. It allows to insert up to 7 semiconductor layers and almost all parameters can be graded (i.e. dependent on the optical composition or on the depth in the cell) *Eg, χ, ε, NC, NV, vthn, vthp, μn, μp, NA, ND,* all traps (defects) *Nt.* Recombination mechanisms are band-to-band (direct), Auger, SRH-type. Defect levels are in bulk or at interface; their charge state and recombination is accounted for defect levels. Charge types are no charge (idealization), monovalent (single donor, acceptor), divalent (double donor, double acceptor, amphoteric), multivalent (user defined) defect levels. Energetic distributions are single level, uniform, Gauss, tail, or combinations defect levels. Optical property is direct excitation with light possible (impurity photovoltaic effect, IPV). Meta-stable defects are transitions between acceptor and donor configurations for known meta-stable defects in CIGS: the V_Se and the In_Cu defect; also custom set meta-stable transitions implemented. Metal Contacts consist work function or flat-band; optical property (reflection of transmission filter) filter. It allows two types of tunneling: intra-band tunneling (within a conduction band or within a valence band); tunneling to and from interface states. Generation is created either from internal calculation or from user suppied $G(x)$ file. Illumination consist a variety of standard and other spectra included (AM0, AM1.5D, AM1.5G, AM1.5Gedition2, monochromatic, white). Illumination can be done from either the *p*-side or the *n*-side; spectrum cut-off and attenuation. Working point for calculations are voltage, frequency, temperature. The program calculates energy bands, concentrations and currents at a given working point, *J-V* characteristics, ac characteristics (*C* and *G* as function of *V* and/or *f*), spectral response (also with bias light or voltage). Batch calculations are possible; presentation of results and settings as a function of batch parameters. Loading and saving of all settings; startup of SCAPS in a personalized configuration; a script language including a free user function. SCAPS is very intuitive user interface. A script language facility to run SCAPS from a "script file"; all internal variables can be accessed and plotted via the script. It also provides a built-in curve fitting facility.

3.2. Basic Cell Confirmation

For this thesis, a CIGS cell that was comprised of five layers was constructed. Starting with the top of the cell, the layers are as follows; Al:ZnO-0.2 µm, iZnO-0.1 µm, CdS/In_2S_3/ZnS-0.05 µm, CIGS-2.0 µm, and Mo-0.4 µm. The simulated cell had a top area of one centimeter squared, based on the industry standard for laboratory testing. A visual representation of the base cell structure is depicted in Figure: 4-5.

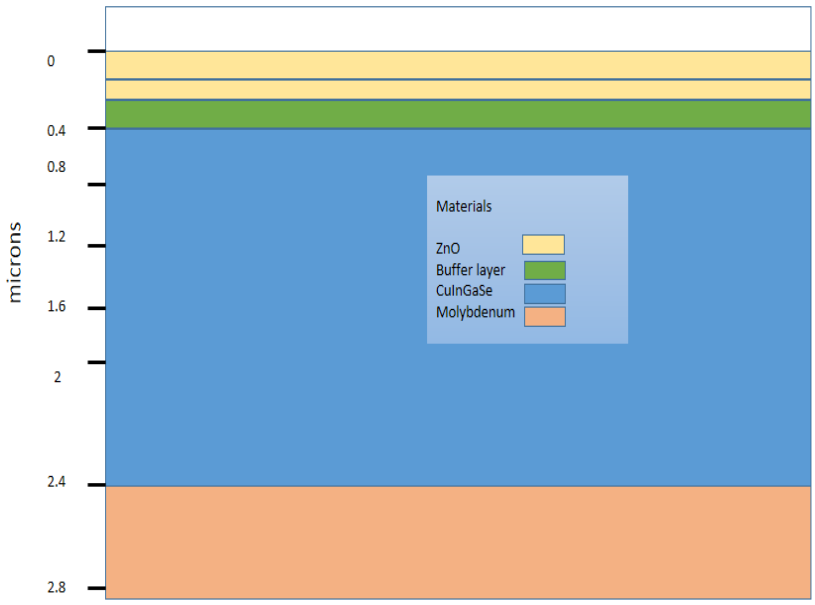

Figure: 3-1 Control cells used as the basis of simulation.

In researching the basic semiconductor parameters for CIGS cells, it was found that the parameters varied only slightly. By putting these parameters into SCAPS the values were calculated automatically according to material parameters and doping. The semiconductor parameters used in this thesis were relative permittivity Er, band gap *Eg*, electron affinity χe, density of states in the conduction band Nc, density states in valence band Nv, electron band mobility µn, and hole band mobility µp. The parameters of conventional CIGS solar cell inputted into SCAPS are displayed in Table 3-1.

3.3 CIGS Absorber Layer:

The suitability of thin-film Cu(In,Ga)(Se)2 (CIGS) absorber layer in solar cell (SCs) usage is shown in many studies because these chalcopyrite compounds have shown the highest efficiencies for laboratory thin film SCs. The semiconductor CIGSS material have a high value of absorption index, therefore, it is possible to use a fairly thin films in absorber layer of solar cell. This, in turn, significantly reduces material costs.

3.3.1 Parameters:

The semiconductor parameters band gap E_g, relative permittivity ε_r, electron affinity χ_e, density of states in the conduction band N_c, density states in valence band N_v, electron band mobility μ_n, and hole band mobility μ_p for CIGS absorber layer is shown in Table-1.

Table: 3-1 Semiconductor material parameters of CIGS absorber layer

Bandgap (eV)	1.24
Electron Affinity (eV)	4.5
Dielectric Permittivity	13.6
CB effective density of states (1/cm3)	2.2E+18
VB effective density of states (1/cm3)	1.8E+19
Electron Thermal velocity (cm/s)	3.9E+7
Hole Thermal velocity (cm/s)	1.4E+7
Electron mobility (cm2/Vs)	1.0E+2
Hole mobility (cm2/Vs)	2.5E+1

The cell used as the base line was given a Ga content of 30%. This yielded a cell that had a band gap of 1.24eV.

3.3.2 Thickness Optimization:

It was developed many methods to produce thin films of CIGS. Depending on the production method the following photoactive layer thicknesses are possible: ~1.5 µm for vacuum deposition ~2.0 µm for co-evaporation in vacuum ~2.0 µm for metallic precursors handling in Se-vapor.

Since the CIGS solid solution allows production of thin enough SCs, there is a need to clarify the optimal value of the thickness of the absorbing layer in SCs based on CIGS. Too small thickness of the absorbing layer leads to a lower value of the photocurrent. Too thick absorbing layer leads to a large series resistance and increase in material consumption and, consequently, the cost per unit of power produced.

In this thesis we consider the influence of the photoactive layer thickness on photocurrent for a CIGS based SC. The thickness of the CIGS absorber layer are optimized for four thickness parameters and the parameters are varied from 1um to 2.5um with an interval of .5um. The individual sweep with different thickness is shown below:

The first sweep was done with 1um of absorber layer. Simulating in SCAPS, the result shows that the value of short circuit current, J_{SC} is 0.426 mA/cm2, open circuit voltage, V_{OC} 0.6332V and fill factor 80.20%.

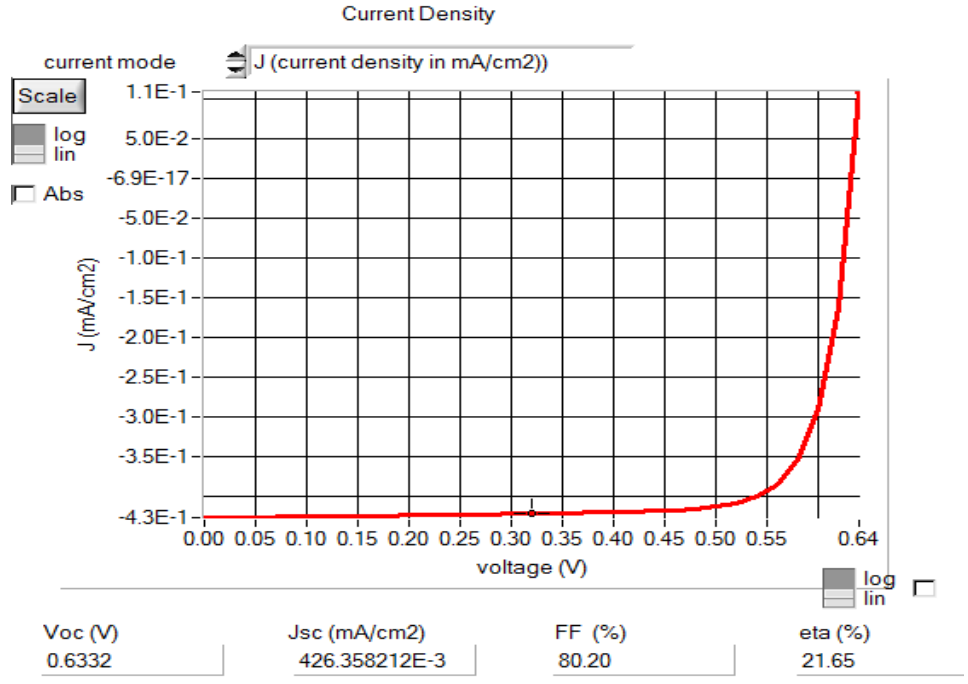

Figure: 3-2 J_{SC} and V_{OC} of CIGS solar cell with 1um thickness of CIGS absorber layer and corresponding efficiency.

The second sweep was done with 1.5um of absorber layer. Simulating in SCAPS, the result shows that the value of short circuit current, J_{SC} is 0.444 mA/cm2, open circuit voltage, V_{OC} 0.6329V and fill factor 80.40%.

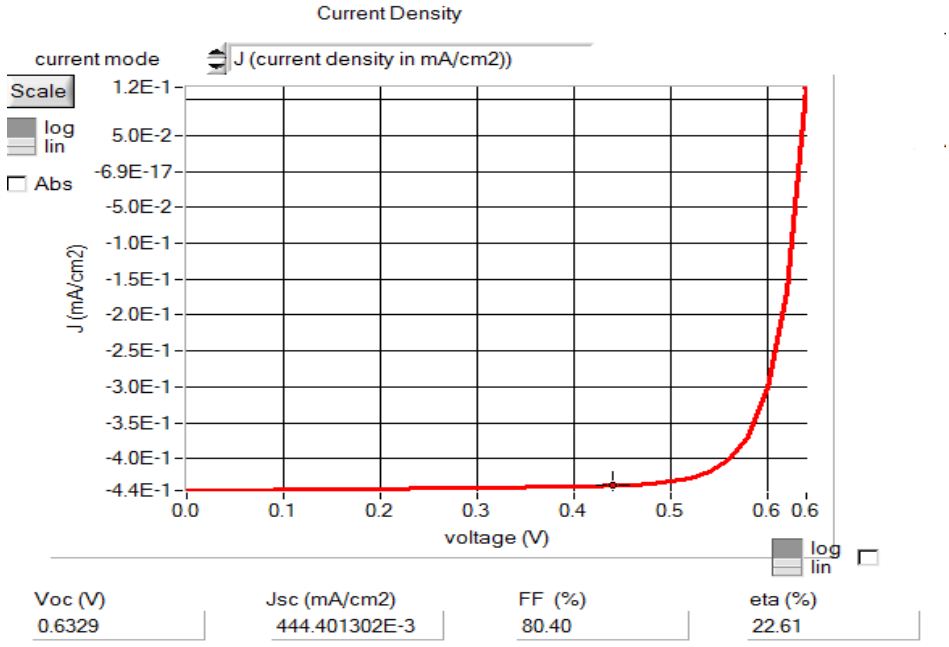

Figure: 3-3 J_{SC} and V_{OC} of CIGS solar cell with 1.5um thickness of CIGS absorber layer and corresponding efficiency.

The third sweep was done with 2um of absorber layer. Simulating in SCAPS, the result shows that the value of short circuit current, J_{SC} is 0.460 mA/cm2, open circuit voltage, V_{OC} 0.6406V and fill factor 80.54%.

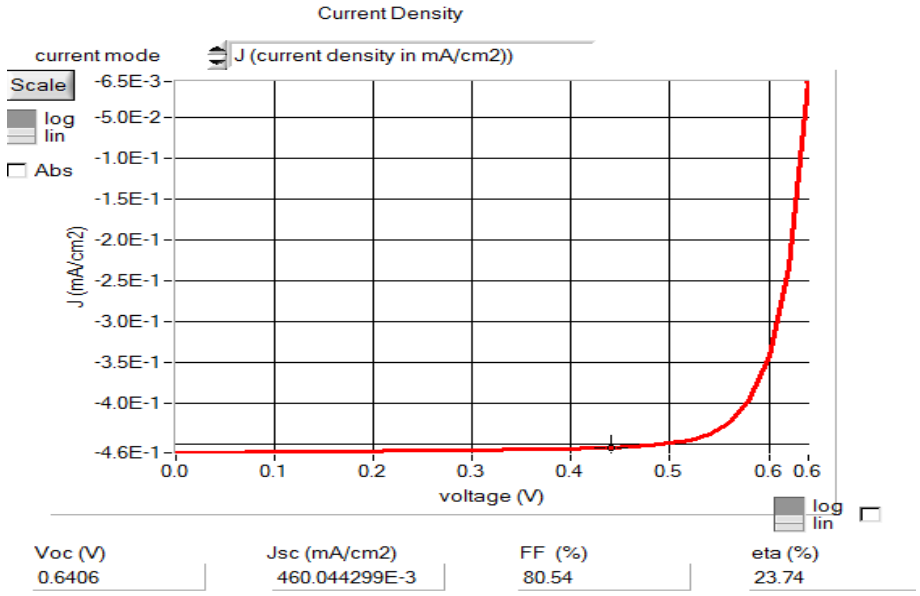

Figure: 3-4 J_{SC} and V_{OC} of CIGS solar cell with 2um thickness of CIGS absorber layer and corresponding efficiency.

The fourth sweep was done with 2.5um of absorber layer. Simulating in SCAPS, the result shows that the value of short circuit current, J_{SC} is 0.472 mA/cm2, open circuit voltage, V_{OC} 0.6489V and fill factor 80.30%.

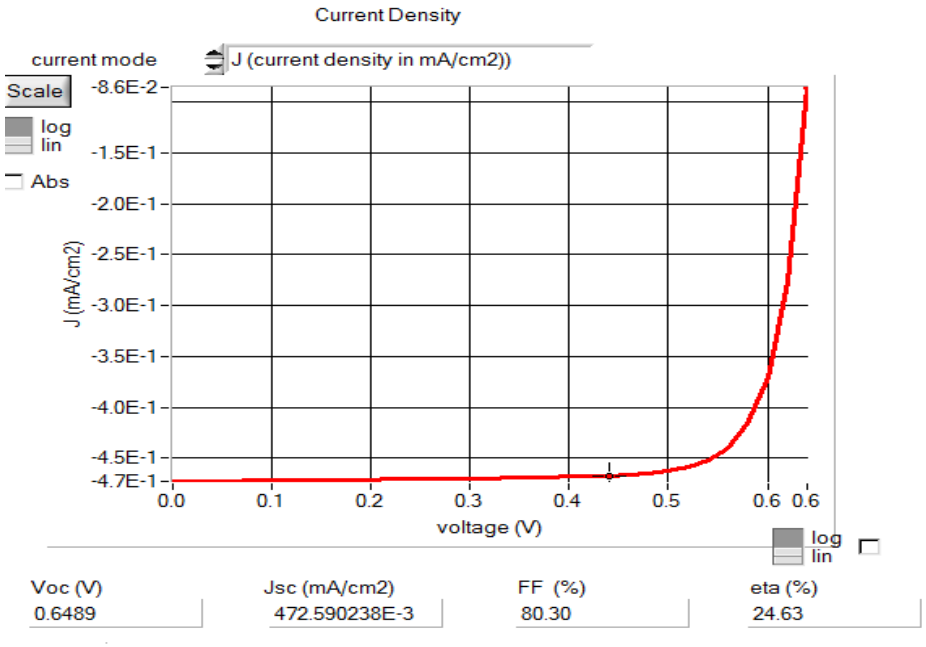

Figure: 3-5 J_{SC} and V_{OC} of CIGS solar cell with 2.5um thickness of CIGS absorber layer and corresponding efficiency.

From sweeping results, it can be seen that cell efficiency continues to increase as the CIGS thickness increases. As the thickness of the absorber layer is increased, more carriers are generated. More carriers results in higher I_{SC} and a higher current at the maximum power point. As the CIGS layer increases, carriers generated farther from the p-n junction are subjected to a weaker electric field and more subject to recombination of electrons and holes. This recombination results in a law of diminishing returns where an increase of layer thickness does not result in major efficiency gains. The thickness of CIGS was capped at 2.5 µm to prevent chasing higher efficiency at the cost of losing the lightweight flexible qualities.

Table: 3-2 Comparison of I-V characteristics, fill factors and efficiencies w.r.t CIGS thickness

	1um	1.5um	2um	2.5um
J_{SC} (mA/cm2)	0.426	0.444	0.460	0.472
V_{OC} (V)	0.6332	0.6329	0.6406	0.6489
FF (%)	80.20	80.40	80.54	80.30
n (%)	21.65	22.61	23.74	24.63

3.3.3 Bandgap Optimization:

According to the theoretical considerations proposed by Loferski and also based on Shockley–Queisser limit, the maximum theoretical efficiency of a solar cell can be obtained by the absorber layer band gap in the range of 1.2 eV to 1.5 eV (Loferski, 1956; Shockley & Queisser, 1961). This has led to the interest in using CIGS material due to its energy band gap, which is in the range of 1.04 eV to 1.69 eV. This feature firmly makes CIGS as a promising semiconductor material to be used as an absorber layer in a thin film solar cell [41].

Continuing from the base cell, the method in which SCAPS calculated band gap needed to be verified. Five cells with different band gaps were modeled in this thesis. The amount of Ga used in the five cells was 0%, 10%, 30%, 50%, and 70%. Each Ga content was entered separately and calculated from the equation below. The calculated band gaps from lowest to highest were 1.04 eV, 1.15 eV, 1.24 eV, 1.41 eV and 1.55 eV. Performing a quadratic regression on this data yielded a band gap equation of

$$E_g\ (eV) = 0.024x^2 + 0.667x + 1.07$$

Where x is the mole fraction of Ga used in the CIGS region. An extrapolated curve of this data is shown in Figure.

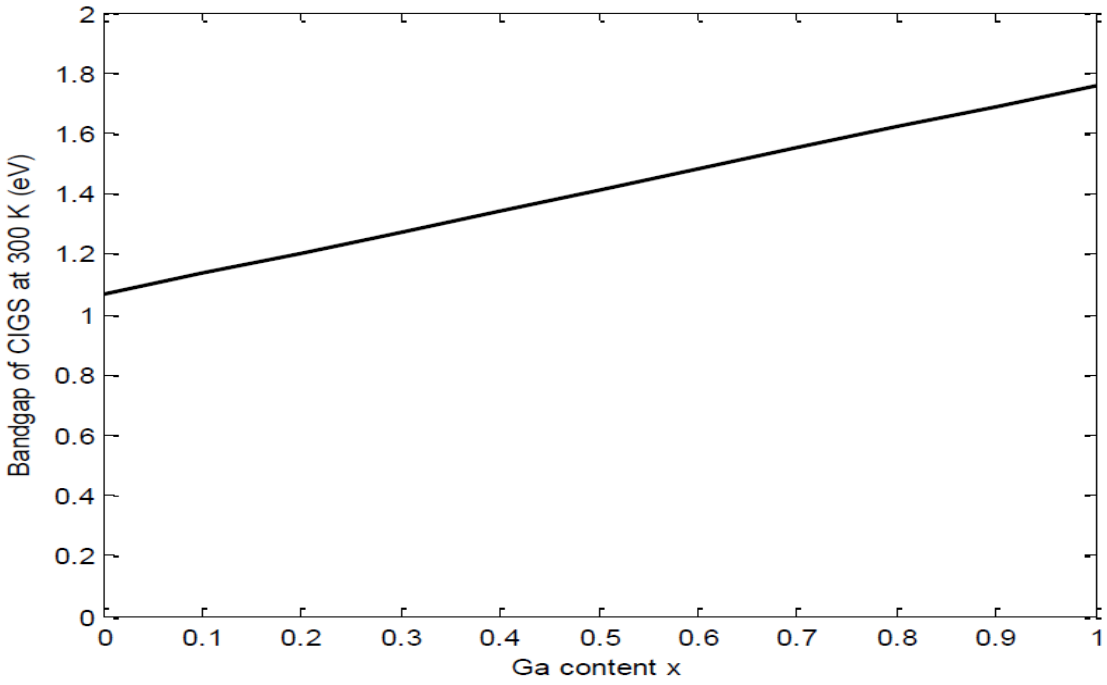

Figure: 3-6 Extrapolated graph of Ga content versus band gap.

The first sweep was done with a bandgap of 1.04eV (0% Ga content). Simulating in SCAPS, the result shows that the value of short circuit current, J_{SC} is 0.460 mA/cm2, open circuit voltage, V_{OC} 0.4405V and fill factor 75.70% which corresponds to an efficiency of 15.37%.

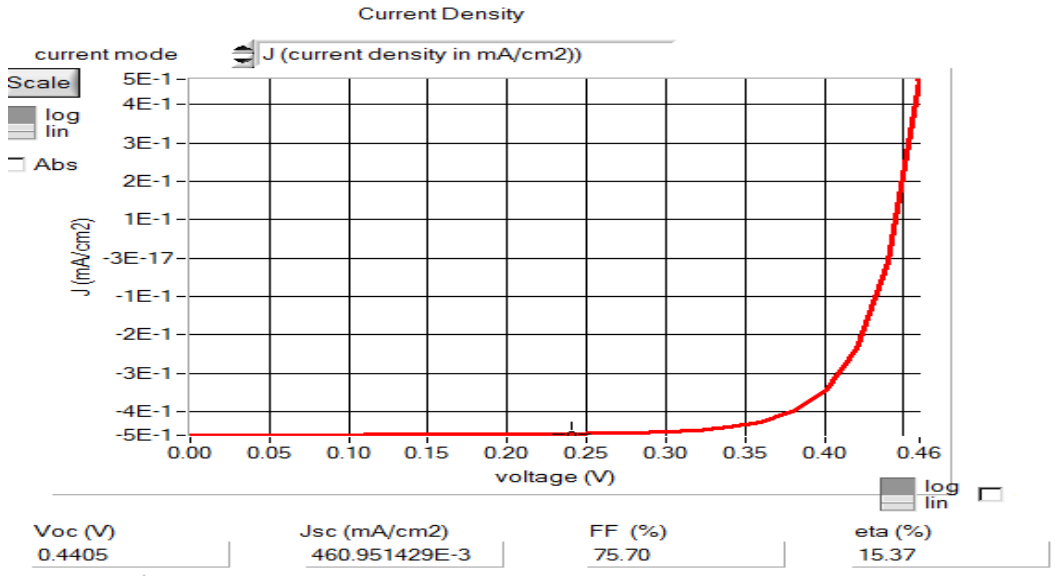

Figure: 3-7 J_{SC} and V_{OC} of CIGS solar cell with 0% Ga content (bandgap 1.04ev) and corresponding efficiency.

The second sweep was done with a bandgap of 1.15eV (10% Ga content). Simulating in SCAPS, the result shows that the value of short circuit current, J_{SC} is 0.462 mA/cm2, open circuit voltage, V_{OC} 0.5500V and fill factor 78.80% which corresponds to an efficiency of 20.03%.

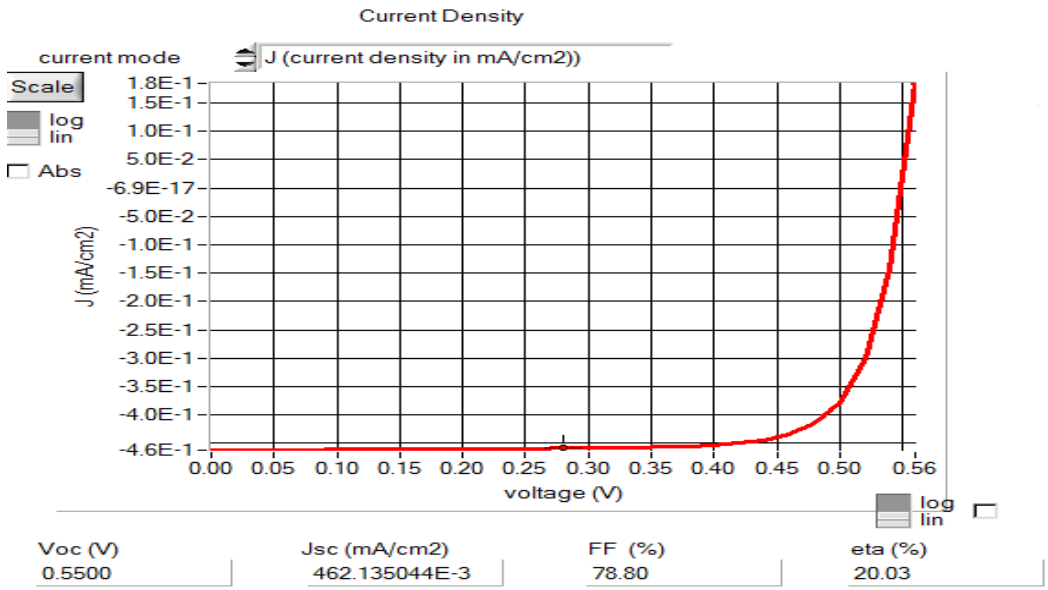

Figure: 3-8 J_{SC} and V_{OC} of CIGS solar cell with 10% Ga content (bandgap 1.15ev) and corresponding efficiency.

The third sweep was done with a bandgap of 1.24eV (30% Ga content). Simulating in SCAPS, the result shows that the value of short circuit current, J_{SC} is 0.460 mA/cm2, open circuit voltage, V_{OC} 0.6406V and fill factor 80.54% which corresponds to an efficiency of 23.74%.

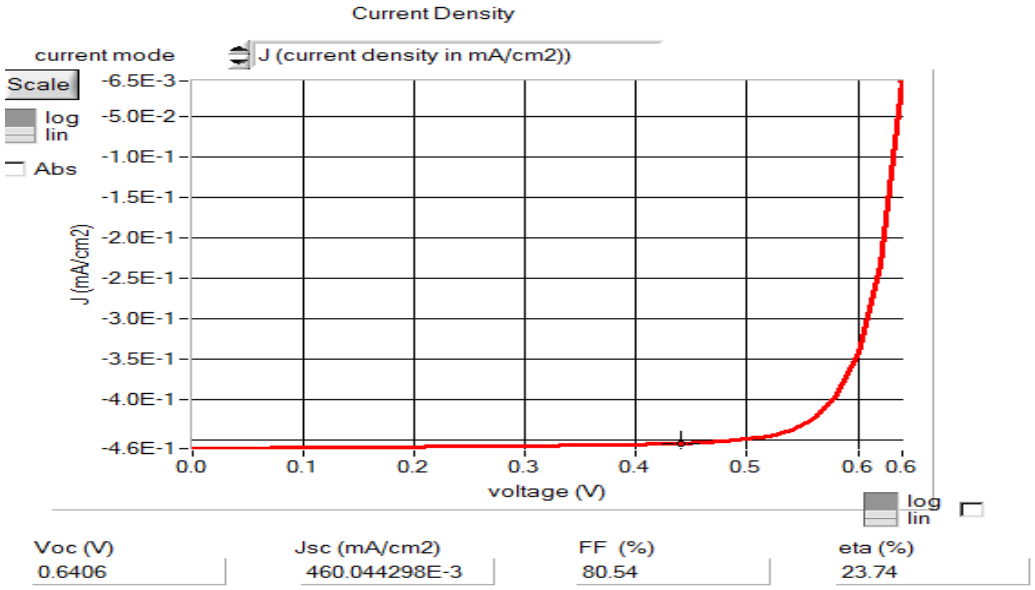

Figure: 3-9 J_{SC} and V_{OC} of CIGS solar cell with 30% Ga content (bandgap 1.24ev) and corresponding efficiency.

The fourth sweep was done with a bandgap of 1.41eV (50% Ga content). Simulating in SCAPS, the result shows that the value of short circuit current, J_{SC} is 0.460 mA/cm2, open circuit voltage, V_{OC} 0.9348V and fill factor 61.12% which corresponds to an efficiency of 26.31%.

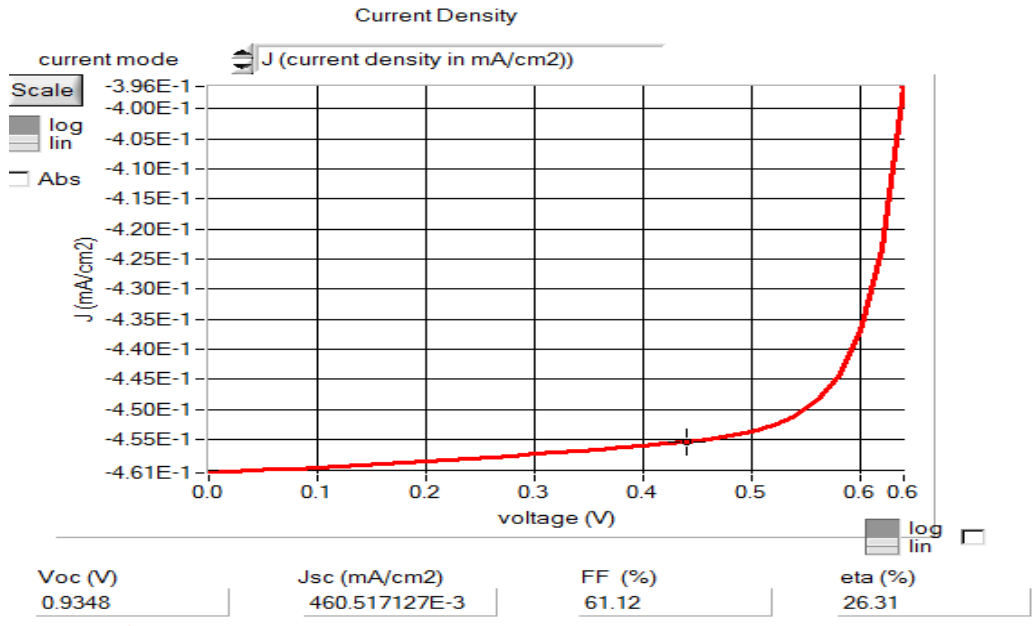

Figure: 3-10 J_{SC} and V_{OC} of CIGS solar cell with 50% Ga content (bandgap 1.41ev) and corresponding efficiency

The fifth sweep was done with a bandgap of 1.55eV (70% Ga content). Simulating in SCAPS, the result shows that the value of short circuit current, J_{SC} is 0.463 mA/cm2, open circuit voltage, V_{OC} 1.0717V and fill factor 54.18% which corresponds to an efficiency of 26.92%.

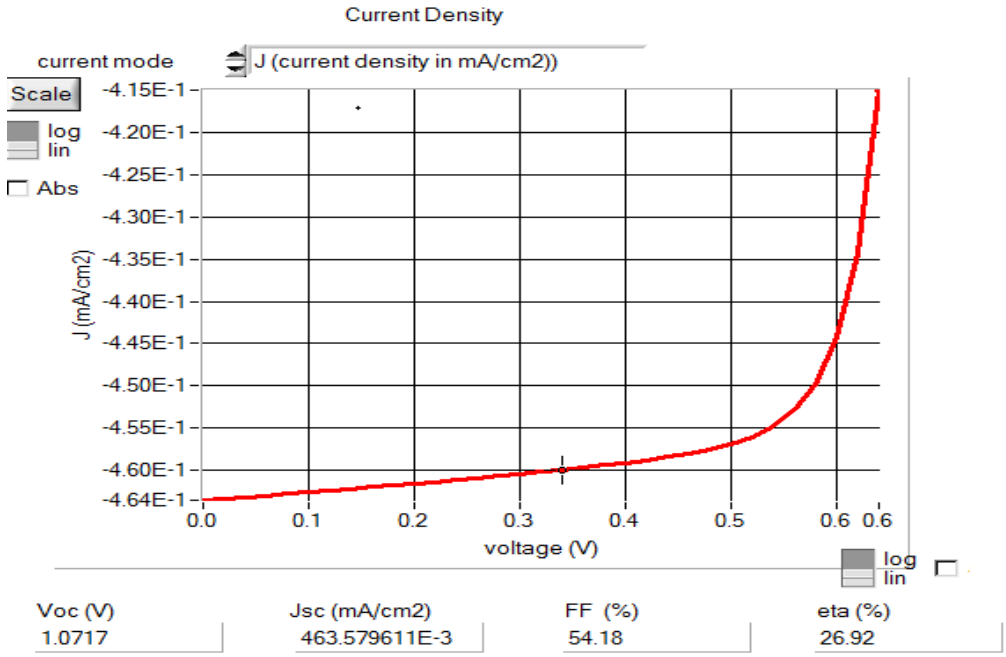

Figure: 3-11 J_{SC} and V_{OC} of CIGS solar cell with 70% Ga content (bandgap 1.55ev) and corresponding efficiency.

In addition to recording the calculated band gaps, IV curves for each of the five cells were obtained. Comparing the IV curves of cells with differing band gaps ensured that SCAPS was successfully modeling higher band gaps material. Higher band gap solar cells should produce a higher V_{OC} but a lower I_{SC}. The five IV curves of the control cell with different badgaps are shown in the sweeping Figures. A detailed breakdown of the data from Figures is given in Table: 3-3.

Table: 3-3 Comparison of I-V characteristics, fill factors and efficiencies w.r.t CIGS bandgap

	1.04eV	1.15eV	1.24eV	1.41eV	1.55eV
J_{SC} (mA/cm2)	0.460	0.462	0.460	0.460	0.463
V_{OC} (V)	0.4405	0.5500	0.6406	0.9348	1.0717
FF (%)	75.70	78.80	80.54	61.12	54.18
n (%)	15.37	20.03	23.74	26.31	26.92

3.4 Buffer layer Optimizations:

The other important layer of the CIGS solar cell structure is the buffer layer. The role of a buffer layer in a heterojunction is to form a junction with the absorber layer, while leading maximum amount of incoming light to the absorber layer. The buffer layer should have minimal absorption losses, low surface recombination and minimal electrical resistance when transporting the photo generated carriers to the outer circuit (McCandless & Hegedus, 1991). The most important features of the buffer layer are protecting the junction against the chemical reactions and mechanical damage, as well as optimizing the band alignment of the cell, electrical properties and making a wide depletion region with the p-type absorber layer. This eventually can minimize the carriers tunneling and maintain higher open circuit voltage value to establish higher contact potential (Contreras *et al*., 2002). In order to satisfy such desired features, the buffer layer should have a wider band gap in comparison with the CIGS layer.

In this thesis, we've optimized the CIGS solar cell for three different buffer layers:

i. **Cadmium Sulfide (CdS)**
ii. **Indium Sulfide (In_2S_3)**
iii. **Zinc Sulfide (ZnS)**

3.4.1 CdS buffer layer:

The most common used material as a buffer layer in CIGS solar cells is Cadmium Sulfide (CdS). Cadmium sulfide (CdS) with direct band gap (2.4 eV at room temperature) is an n-type semiconductor. It is one of the most promising materials for application in different optoelectronic and photovoltaic devices like photo-sensors, photo conducting sensors, biological labels, and high-efficiency copper-indium-gallium-selenide (CIGS) solar cells. Various methods are utilized to deposit CdS thin films, such as sol–gel, spray pyrolysis, pulsed laser deposition, laser beam sputtering, chemical vapor deposition (CVD), and chemical bath deposition (CBD) [42]. CBD is applied intensively for deposition of CdS thin layers on different substrates due to its low cost and simplicity. On the other hand, the CBD method leads to the formation of a large amount of hazardous solvent waste. Therefore, it would be interesting to use another technique that requires less material, which would lower the waste material and processing cost. This study includes the preparation of a liquid coating solution that will be applied on the heated substrate surface using a hot plate.

3.4.1.1 Parameters:

The semiconductor parameters band gap E_g, relative permittivity ε_r, electron affinity χ_e, density of states in the conduction band N_c, density states in valence band N_v, electron band mobility μ_n, and hole band mobility μ_p for CIGS absorber layer is shown in Table: 3-4. The defect properties are shown in Table: 3-5 and the interface between CIGS absorber and CdS buffer layer are shown in Table: 3-6.

Table: 3-4 Semiconductor material parameters of CdS buffer layer

Bandgap (eV)	2.4
Electron Affinity (eV)	4.2
Dielectric Permittivity	10.0
CB effective density of states (1/cm3)	2.2E+18
VB effective density of states (1/cm3)	1.8E+19
Electron Thermal velocity (cm/s)	3.1E+7
Hole Thermal velocity (cm/s)	1.6E+7
Electron mobility (cm2/Vs)	1.0E+2
Hole mobility (cm2/Vs)	2.5E+1

Table: 3-5 Defect properties of CdS buffer layer

Energetic distribution	Gaussian
Defect Type	Acceptor
Capture Cross section electrons (cm2)	1.00E-15
Capture Cross section holes (cm2)	5.00E-13

Table: 3-6 Interface properties of CIGS/CdS layers

Interface	CIGS/CdS
Defect Type	Acceptor
Capture Cross Section Electrons (cm2)	1.00E-14
Capture Cross Section Holes (cm2)	1.00E-14

3.4.1.2 Thickness Optimization:

The first sweep was done with 0.04um of buffer layer. Simulating in SCAPS, the result shows that the value of short circuit current, J_{SC} is 0.463 mA/cm2, open circuit voltage, V_{OC} 0.6408V and fill factor 80.54%.

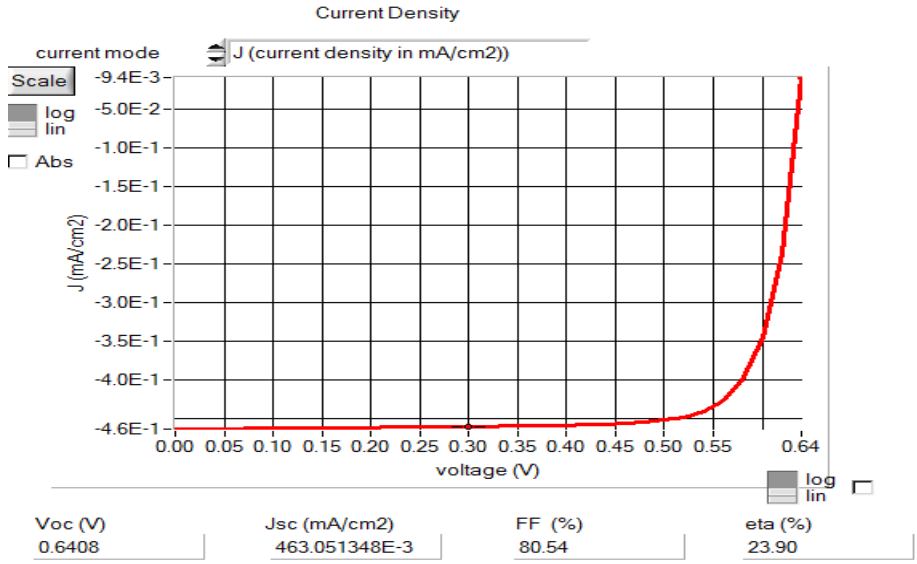

Figure: 3-12 J_{SC} and V_{OC} of CIGS solar cell with CdS buffer layer of .04um thickness and corresponding efficiency

The second sweep was done with 0.05um of buffer layer. Simulating in SCAPS, the result shows that the value of short circuit current, J_{SC} is 0.460 mA/cm2, open circuit voltage, V_{OC} 0.6406V and fill factor 80.54%.

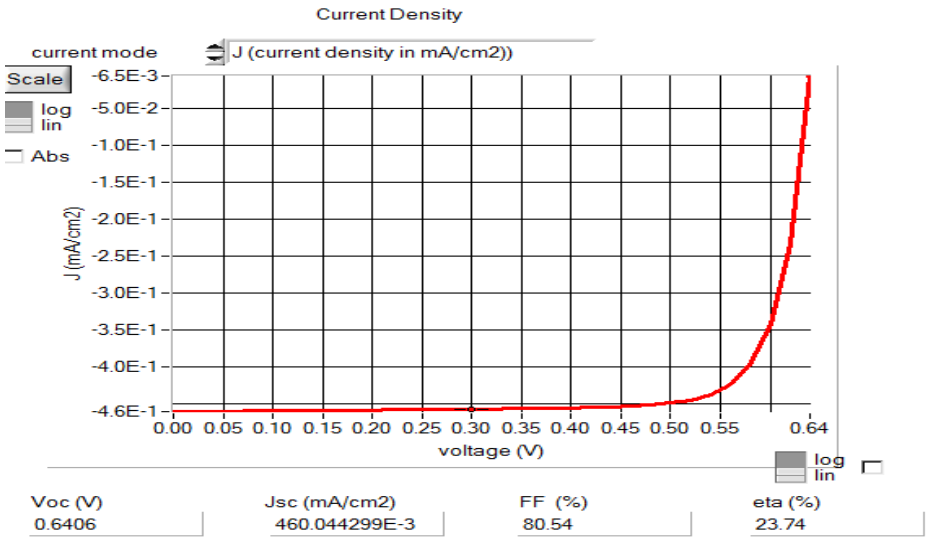

Figure: 3-13 J_{SC} and V_{OC} of CIGS solar cell with CdS buffer layer of .05um thickness and corresponding efficiency

The third sweep was done with 0.06um of buffer layer. Simulating in SCAPS, the result shows that the value of short circuit current, J_{SC} is 0.457 mA/cm2, open circuit voltage, V_{OC} 0.6404V and fill factor 80.55%.

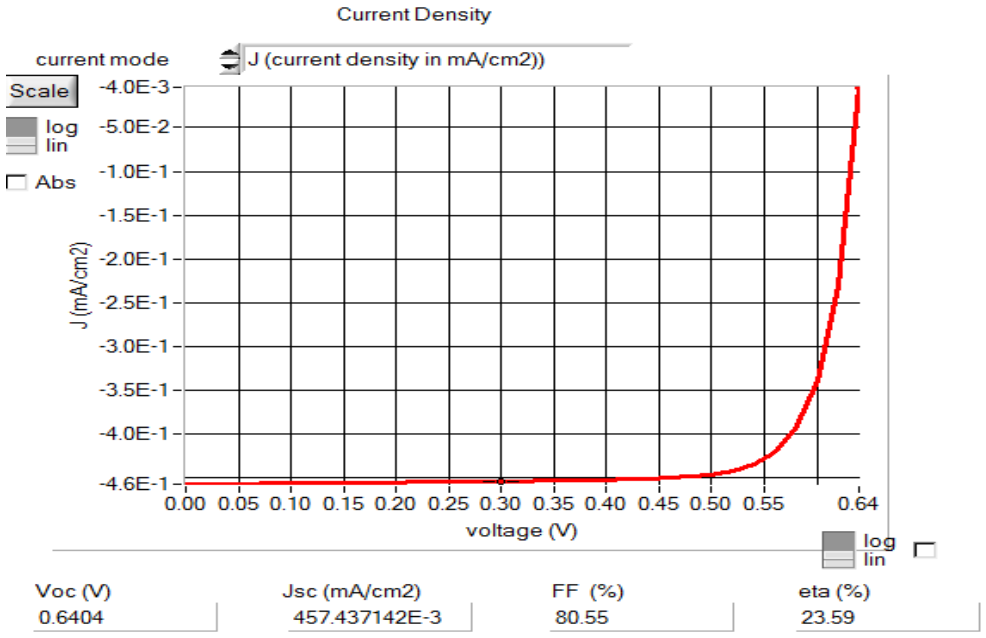

Figure: 3-14 J_{SC} and V_{OC} of CIGS solar cell with CdS buffer layer of .06um thickness and corresponding efficiency

The fourth sweep was done with 0.07um of buffer layer. Simulating in SCAPS, the result shows that the value of short circuit current, J_{SC} is 0.455 mA/cm2, open circuit voltage, V_{OC} 0.6401V and fill factor 80.55%.

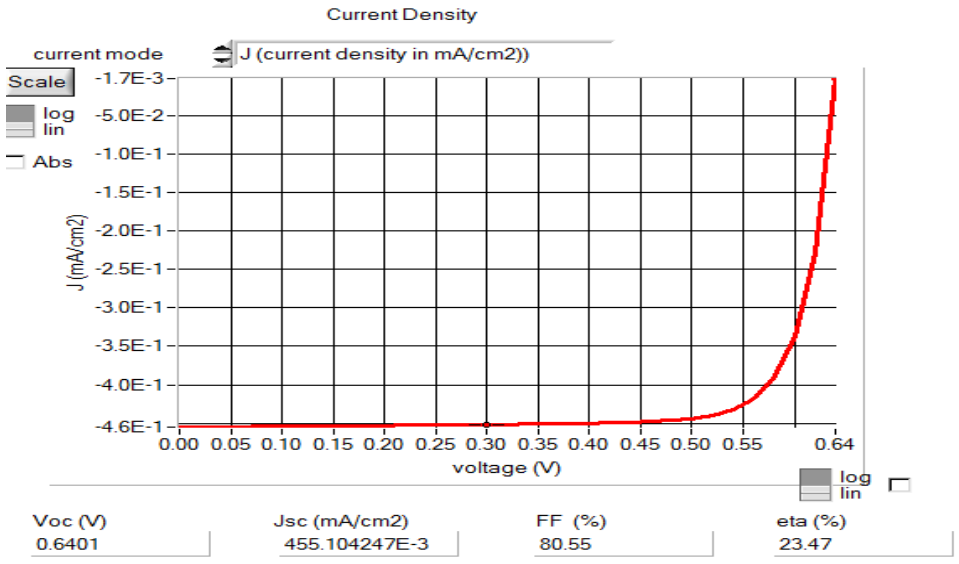

Figure: 3-15 J_{SC} and V_{OC} of CIGS solar cell with CdS buffer layer of .07um thickness and corresponding efficiency

The fifth sweep was done with 0.1um of buffer layer. Simulating in SCAPS, the result shows that the value of short circuit current, J_{SC} is 0.449 mA/cm2, open circuit voltage, V_{OC} 0.6397V and fill factor 80.54%.

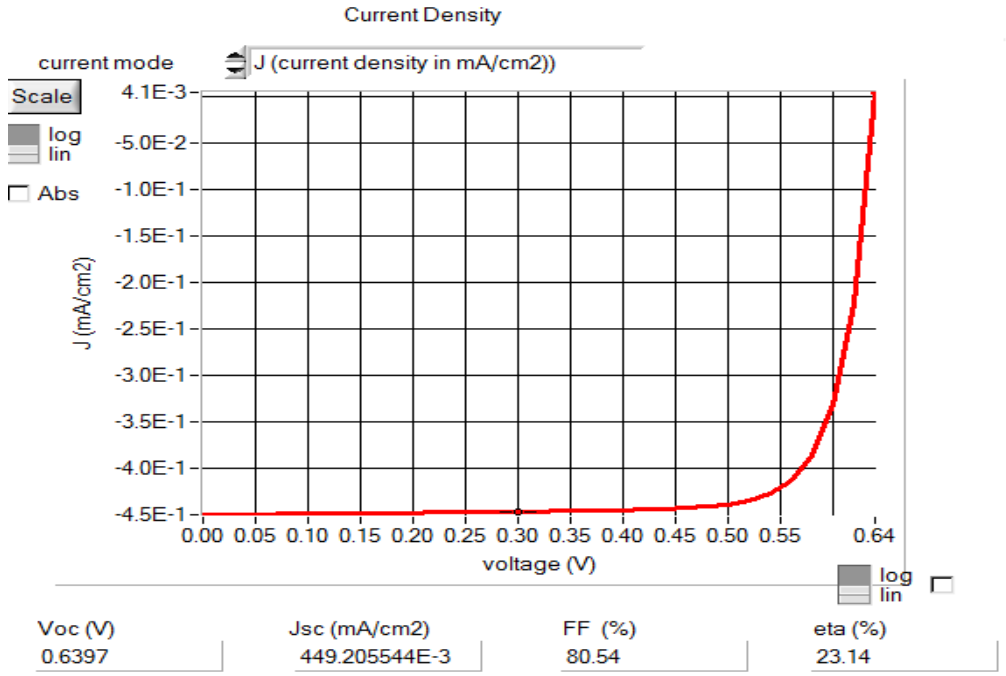

Figure : 3-16 J_{SC} And V_{OC} of CIGS solar cell with CdS buffer layer of .1um thickness and corresponding efficiency

The CIGS cell efficiency is significantly more sensitive to the CdS thickness. Cell efficiency fell over .6% by doubling the thickness of CdS. As stated previously, CdS has a band gap of 2.4 eV. Increasing the thickness CdS creates a stronger electric field between the p-n hetero-junction at the cost of absorbing more of the usable photons from reaching the CIGS layer. From sweeping figures, CdS reached peak efficiency at 0.04 µm. Increasing the thickness efficiency began to fall off.

Table: 3-7 Comparison of I-V characteristics, fill factors and efficiencies w.r.t CdS thickness

	0.04um	0.05um	0.06um	0.07um	0.1um
J_{SC} (mA/cm2)	0.463	0.460	0.457	0.455	0.449
V_{OC} (V)	0.6408	0.6406	0.6404	0.6401	0.6397
FF (%)	80.54	80.54	80.55	80.55	80.54
n (%)	23.90	23.74	23.59	23.47	23.14

3.4.1.3 Quantum Efficiency:

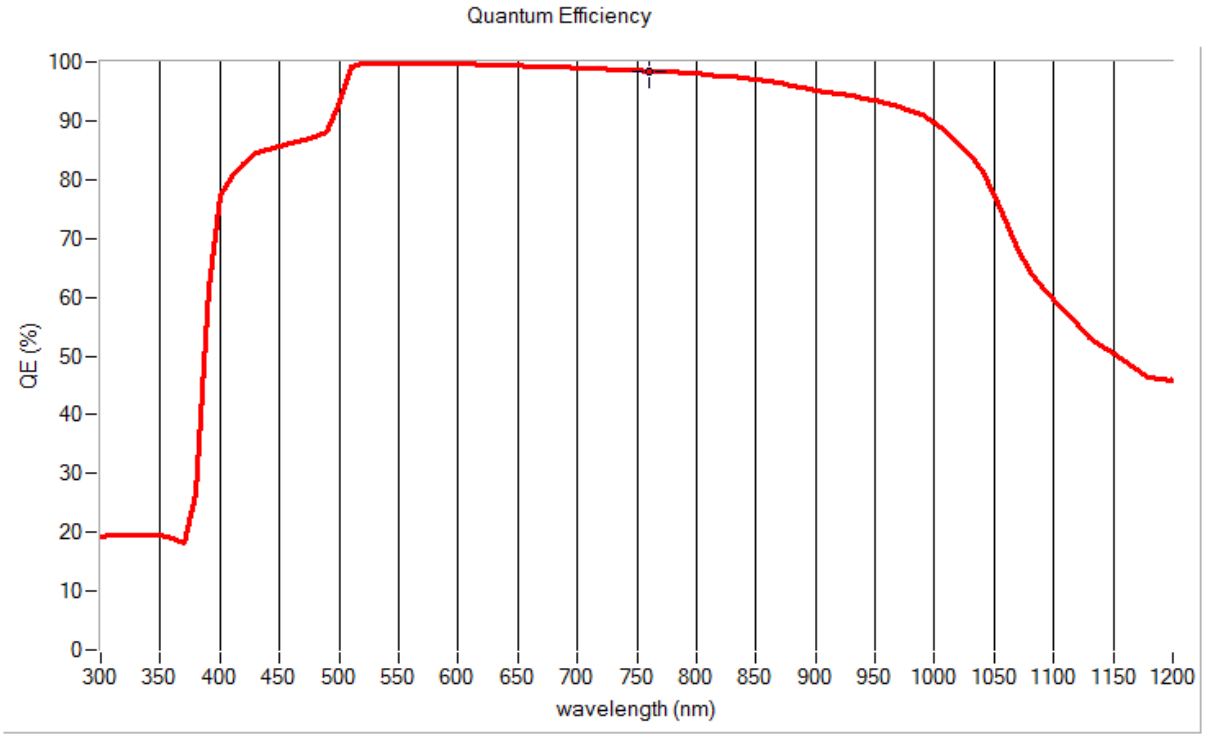

Figure: 3-16 Quantum efficiency of CIGS Solar cell with CdS buffer layer

The external quantum efficiency of a solar cell is shown in Figure: 3-16. The spectral response curve shows a decrease of the long wavelength collection. This is most likely due to incomplete absorption of the long wavelength photons.

For CdS buffer layer the maximum efficiency occurred from 500nm-600nm. The efficiency begin to fall off after 700nm.

3.4.2 In_2S_3 buffer layer:

Cadmium sulfide (CdS) is a prominent candidate to be used a buffer layer in Cu(In,Ga)Se2 based solar cell. Note that Cadmium (Cd) is a metal that can cause severe toxicity in humans and the environment. For this issue, various substitutes have been taken into account as a substitute of CdS buffer layer. Among the other materials, In_2S_3 is considered as an ideal substitute for toxic CdS buffer layer due to its stability, wider band gap (2.1 to 2.8 eV) and photoconductive behavior [43]. Therefore, this In_2S_3 material not only eliminates toxic cadmium but also improve light transmission having band gap wider than that of CdS. The band gap of In_2S_3 can also be increased by partially doping with oxygen or sodium.

3.4.2.1 Parameters:

The semiconductor parameters band gap E_g, relative permittivity ε_r, electron affinity χ_e, density of states in the conduction band N_c, density states in valence band N_v, electron band mobility μ_n, and hole band mobility μ_p for CIGS absorber layer is shown in Table-1. The defect properties are shown in Table-2 and the interface between CIGS absorber and CdS buffer layer are shown in Table-3.

Table: 3-8 Semiconductor material parameters of In_2S_3 buffer layer

Bandgap (eV)	2.1-2.5
Electron Affinity (eV)	4.45
Dielectric Permittivity	13.6
CB effective density of states (1/cm3)	1.8E+19
VB effective density of states (1/cm3)	4.0E+13
Electron Thermal velocity (cm/s)	1.0E+7
Hole Thermal velocity (cm/s)	1.0E+7
Electron mobility (cm2/Vs)	4.0E+2
Hole mobility (cm2/Vs)	2.1E+1

Table: 3-9 Defect properties of In_2S_3 buffer layer

Energetic distribution	Gaussian
Defect Type	Acceptor
Capture Cross section electrons (cm2)	1.00E-15
Capture Cross section holes (cm2)	5.00E-13

Table: 3-10 Interface properties of CIGS/In_2S_3 layers

Interface	CIGS/In_2S_3
Defect Type	Acceptor
Capture Cross Section Electrons (cm2)	1.00E-14
Capture Cross Section Holes (cm2)	1.00E-14

3.4.2.2 Thickness optimization:

The first sweep was done with 0.04um of buffer layer. Simulating in SCAPS, the result shows that the value of short circuit current, J_{SC} is 0.387 mA/cm2, open circuit voltage, V_{OC} 1.4501V and fill factor 41.69%.

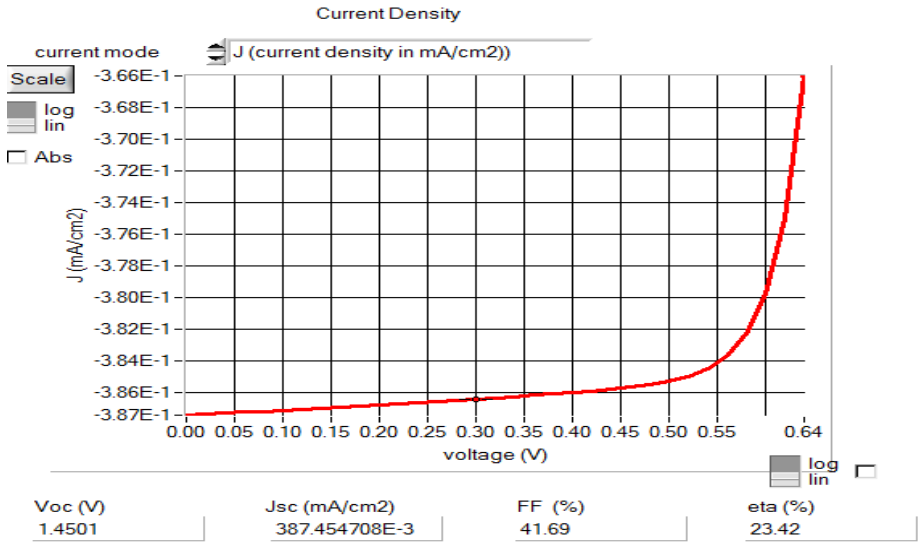

Figure: 3-17 J_{SC} and V_{OC} of CIGS solar cell with In_2S_3 buffer layer of .04um thickness and corresponding efficiency.

The second sweep was done with 0.05um of buffer layer. Simulating in SCAPS, the result shows that the value of short circuit current, J_{SC} is 0.387 mA/cm2, open circuit voltage, V_{OC} 1.4428V and fill factor 41.85%.

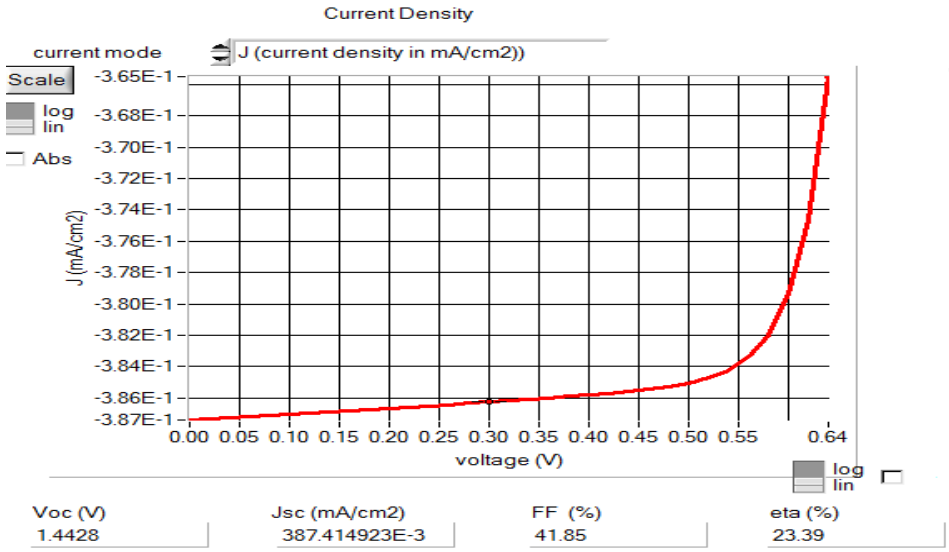

Figure: 3-18 J_{SC} and V_{OC} of CIGS solar cell with In_2S_3 buffer layer of .05um thickness and corresponding efficiency

The third sweep was done with 0.06um of buffer layer. Simulating in SCAPS, the result shows that the value of short circuit current, J_{SC} is 0.387 mA/cm2, open circuit voltage, V_{OC} 1.4403V and fill factor 41.89%.

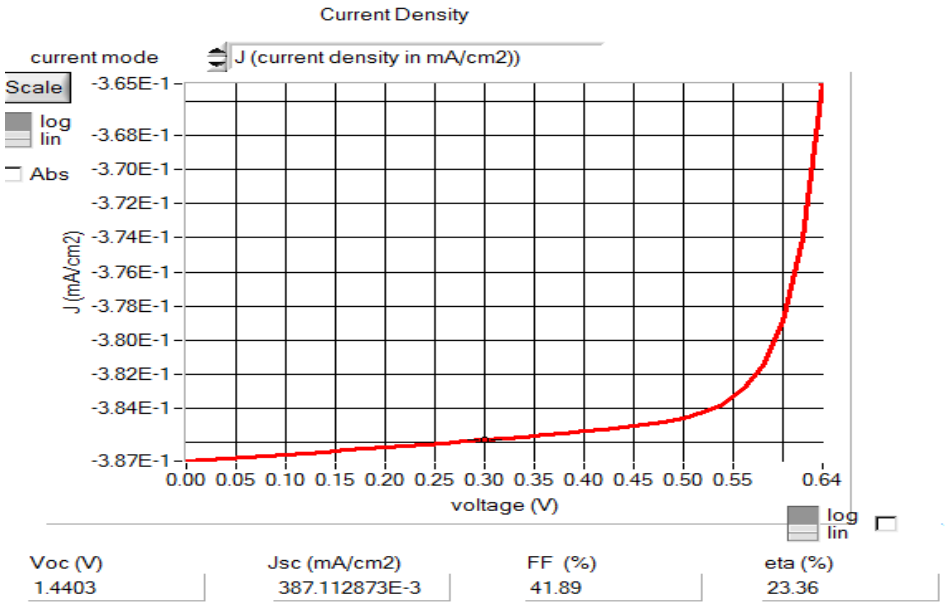

Figure: 3-19 J_{SC} and V_{OC} of CIGS solar cell with In_2S_3 buffer layer of .06um thickness and corresponding efficiency.

The forth sweep was done with 0.07um of buffer layer. Simulating in SCAPS, the result shows that the value of short circuit current, J_{SC} is 0.386 mA/cm2, open circuit voltage, V_{OC} 1.4381V and fill factor 41.93%.

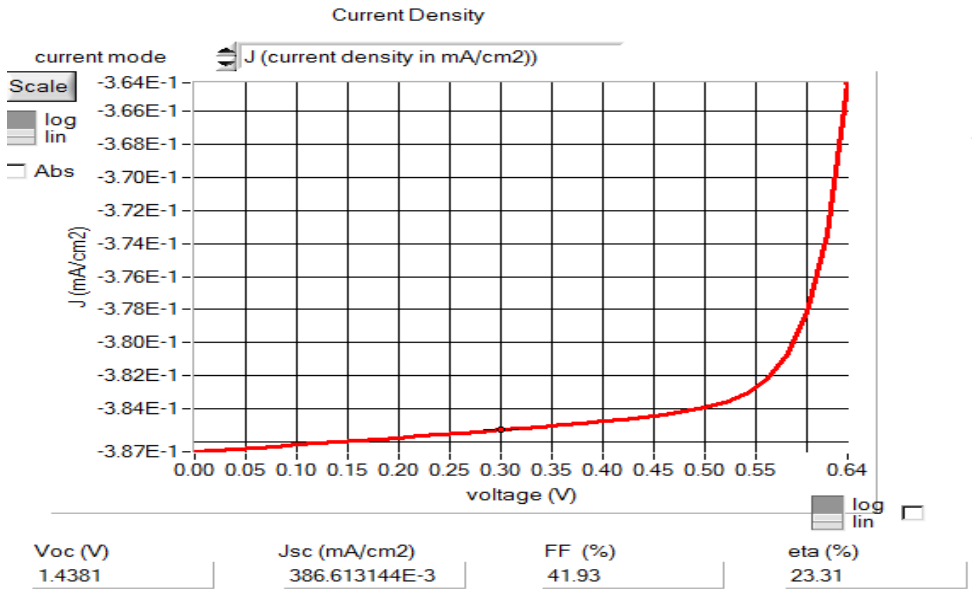

Figure: 3-20 J_{SC} and V_{OC} of CIGS solar cell with In_2S_3 buffer layer of .07um thickness and corresponding efficiency

The fifth sweep was done with 0.1um of buffer layer. Simulating in SCAPS, the result shows that the value of short circuit current, J_{SC} is 0.384 mA/cm2, open circuit voltage, V_{OC} 1.4304V and fill factor 42.09%.

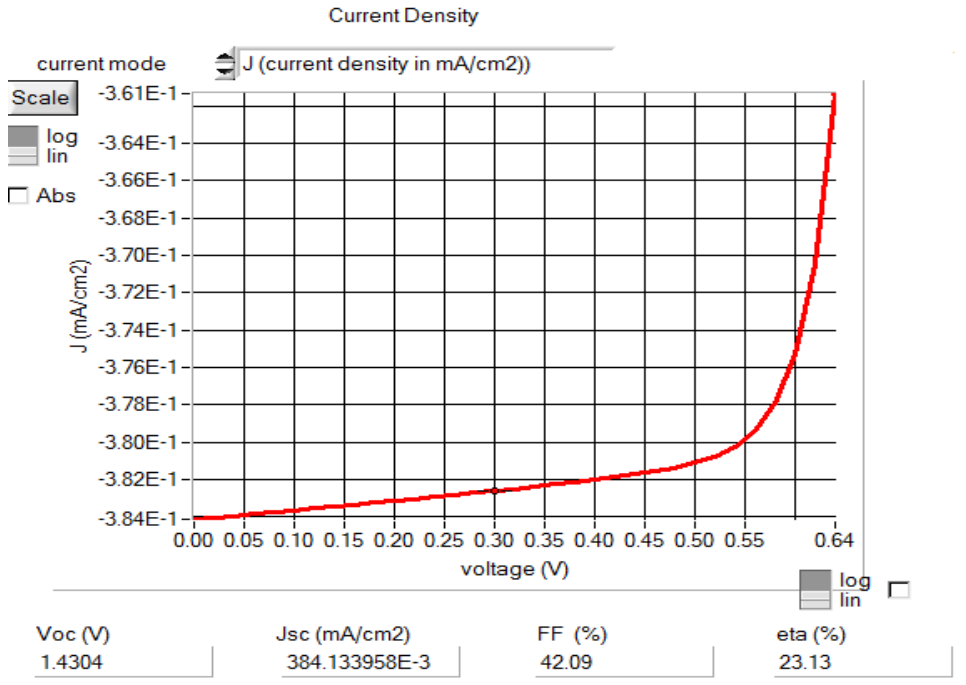

Figure: 3-21 J_{SC} and $V_{OC}$of CIGS solar cell with In_2S_3 buffer layer of .1um thickness and corresponding efficiency

Cell efficiency fell over .3% by doubling the thickness of In_2S_3. As stated previously, In_2S_3 has a band gap of 2.1-2.8 eV. From sweeping figures, In_2S_3 reached peak efficiency at 0.04 µm. Increasing the thickness efficiency began to fall off.

Table: 3-11 Comparison of I-V characteristics, fill factors and efficiencies w.r.t In_2S_3 thickness

	0.04um	0.05um	0.06um	0.07um	0.1um
J_{SC} (mA/cm2)	0.387	0.387	0.387	0.386	0.384
V_{OC} (V)	1.4501	1.4428	1.4403	1.4381	1.4304
FF (%)	41.69	41.85	41.89	41.93	42.09
n (%)	23.42	23.39	23.36	23.31	23.13

3.4.2.3 Quantum Efficiency:

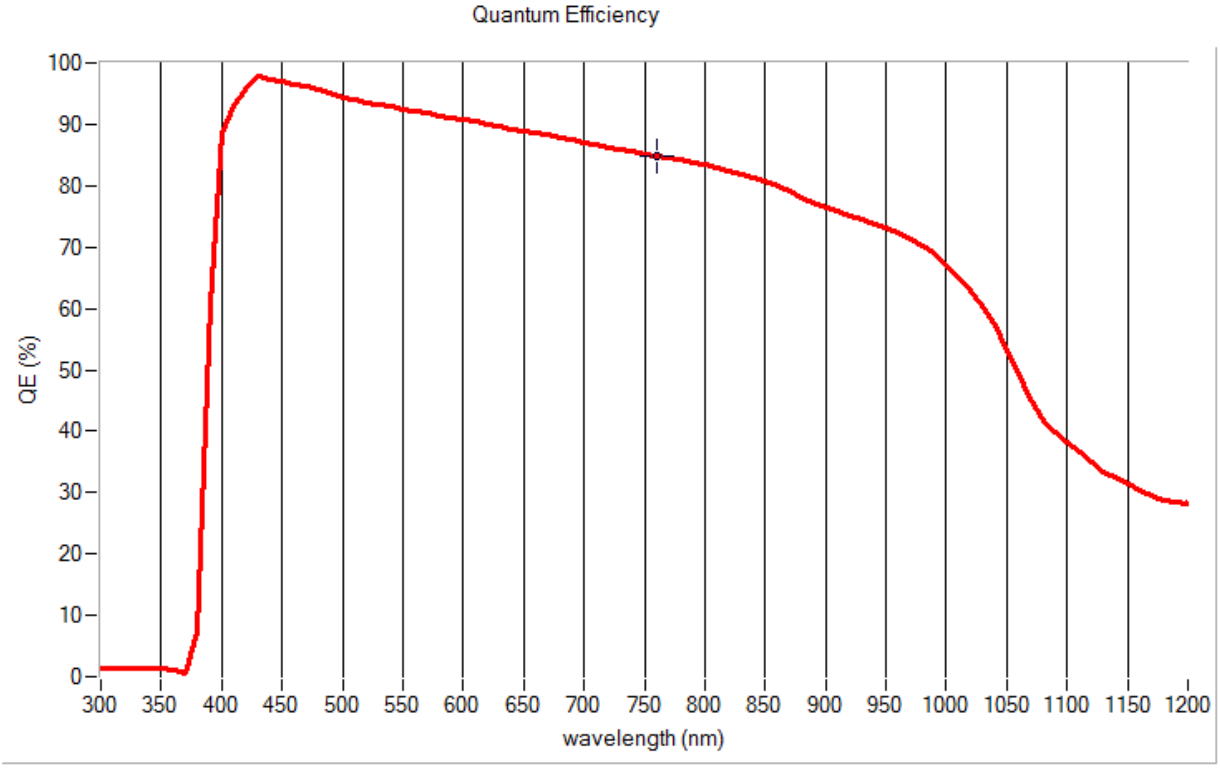

Figure: 3-22 Quantum efficiency of CIGS Solar cell with In_2S_3 buffer layer

The external quantum efficiency of a solar cell is shown in Figure: 3-22. The spectral response curve shows a decrease of the long wavelength collection. This is most likely due to incomplete absorption of the long wavelength photons.

For In_2S_3 buffer layer the maximum efficiency occurred from 400nm-550nm. The efficiency begin to fall off after 600nm.

3.4.3 ZnS buffer layer:

Zinc sulfide is a wide-band-gap semiconductor with a range of potential applications in optoelectronic devices. Generally, in thin film solar cells based on CuInS2, CuInSe2, Cu(In,Ga)Se2, Cu(In,Ga)(SSe)2, (CIGSSe) and comprises of large bandgap of 3.68 eV.

3.4.3.1 Parameters:

The semiconductor parameters band gap E_g, relative permittivity ε_r, electron affinity χ_e, density of states in the conduction band N_c, density states in valence band N_v, electron band mobility μ_n, and hole band mobility μ_p for CIGS absorber layer is shown in Table: 3-12. The defect properties are shown in Table: 3-13 and the interface between CIGS absorber and ZnS buffer layer are shown in Table: 3-14.

Table: 3-12 Semiconductor material parameters of ZnS buffer layer

Bandgap (eV)	3.68
Electron Affinity (eV)	4.13
Dielectric Permittivity	8.9
CB effective density of states (1/cm3)	2.2E+18
VB effective density of states (1/cm3)	1.8E+19
Electron Thermal velocity (cm/s)	1.0E+7
Hole Thermal velocity (cm/s)	1.0E+7
Electron mobility (cm2/Vs)	2.5E+2
Hole mobility (cm2/Vs)	7.0E+1

Table: 3-13 Defect properties of ZnS buffer layer

Energetic distribution	Gaussian
Defect Type	Acceptor
Capture Cross section electrons (cm2)	1.00E-15
Capture Cross section holes (cm2)	5.00E-13

Table: 3-14 Interface properties of CIGS/ZnS layers

Interface	CIGS/ZnS
Defect Type	Acceptor
Capture Cross Section Electrons (cm2)	1.00E-14
Capture Cross Section Holes (cm2)	1.00E-14

3.4.3.2 Thickness Optimization:

The first sweep was done with 0.04um of buffer layer. Simulating in SCAPS, the result shows that the value of short circuit current, J_{SC} is 0.434 mA/cm2, open circuit voltage, V_{OC} 1.4688V and fill factor 40.98%.

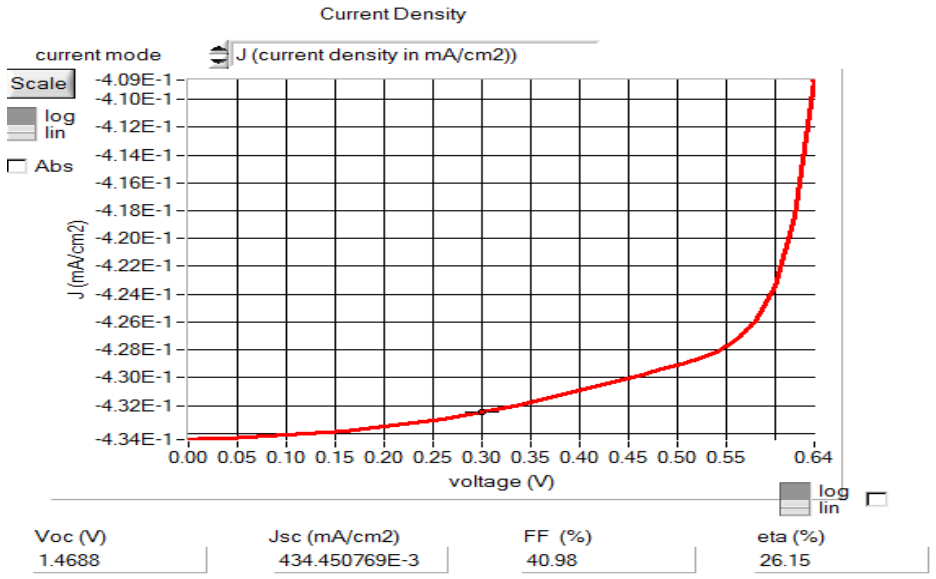

Figure: 3-23 J_{SC} And V_{OC} of CIGS solar cell with ZnS buffer layer of .04um thickness and corresponding efficiency

The second sweep was done with 0.05um of buffer layer. Simulating in SCAPS, the result shows that the value of short circuit current, J_{SC} is 0.431 mA/cm2, open circuit voltage, V_{OC} 1.1212V and fill factor 52.73%.

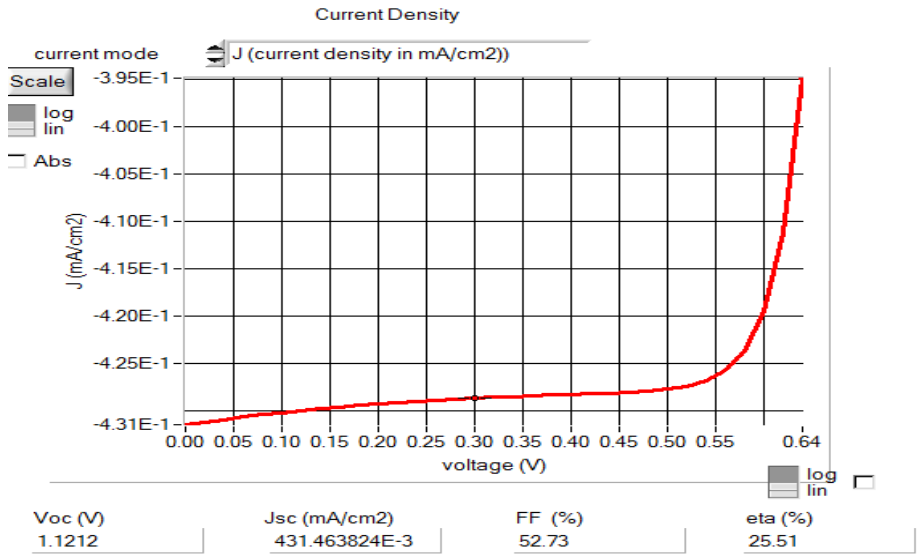

Figure: 3-24 J_{SC} And V_{OC} of CIGS solar cell with ZnS buffer layer of .05um thickness and corresponding efficiency

The third sweep was done with 0.06um of buffer layer. Simulating in SCAPS, the result shows that the value of short circuit current, J_{SC} is 0.428 mA/cm2, open circuit voltage, V_{OC} 1.0502V and fill factor 56.11%.

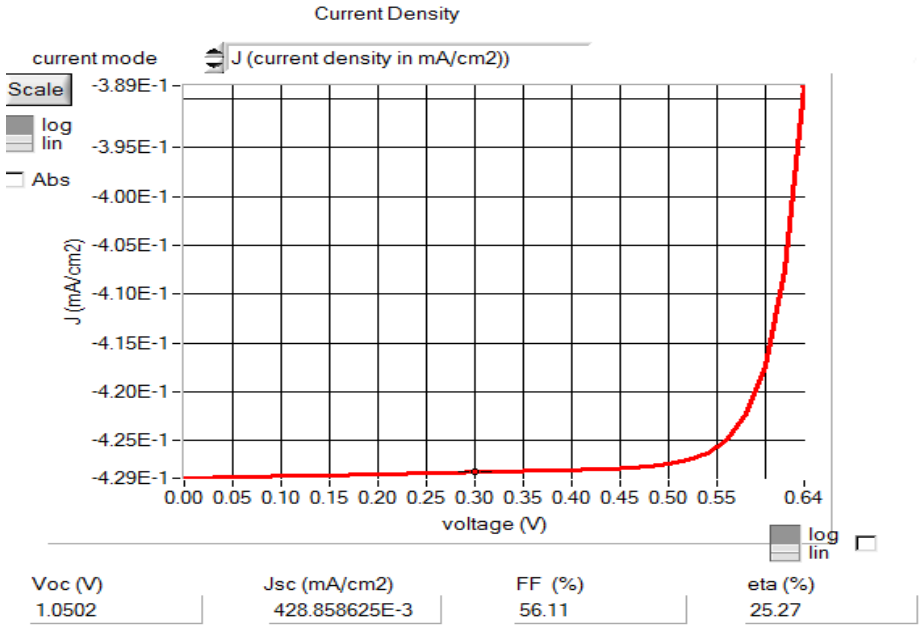

Figure: 3-25 J_{SC} and V_{OC} of CIGS solar cell with ZnS buffer layer of .06um thickness and corresponding efficiency

The fourth sweep was done with 0.07um of buffer layer. Simulating in SCAPS, the result shows that the value of short circuit current, J_{SC} is 0.428 mA/cm2, open circuit voltage, V_{OC} 1.0424V and fill factor 56.48%.

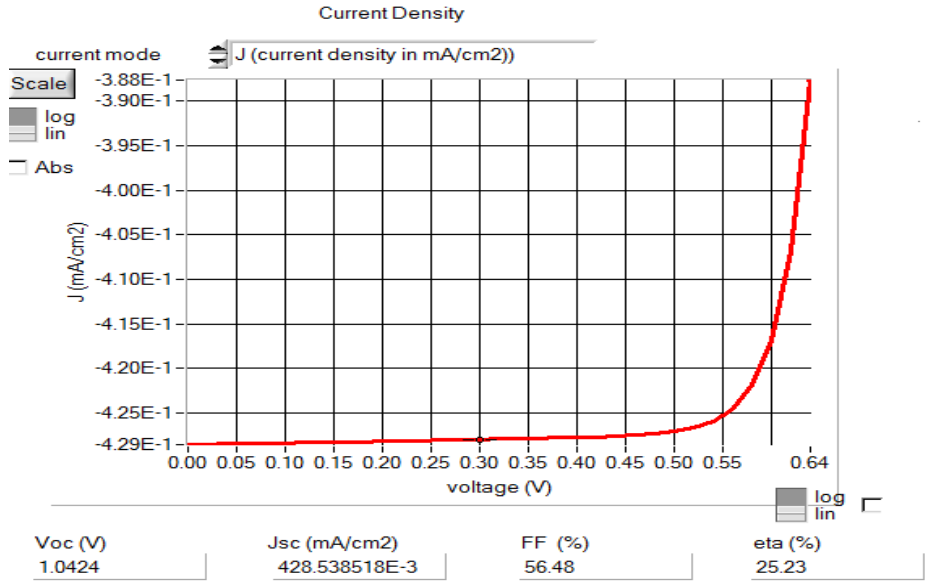

Figure: 3-26 J_{SC} and V_{OC} of CIGS solar cell with ZnS buffer layer of .07um thickness and corresponding efficiency

The fifth sweep was done with 0.1um of buffer layer. Simulating in SCAPS, the result shows that the value of short circuit current, J_{SC} is 0.427 mA/cm2, open circuit voltage, V_{OC} 1.0403V and fill factor 56.57%.

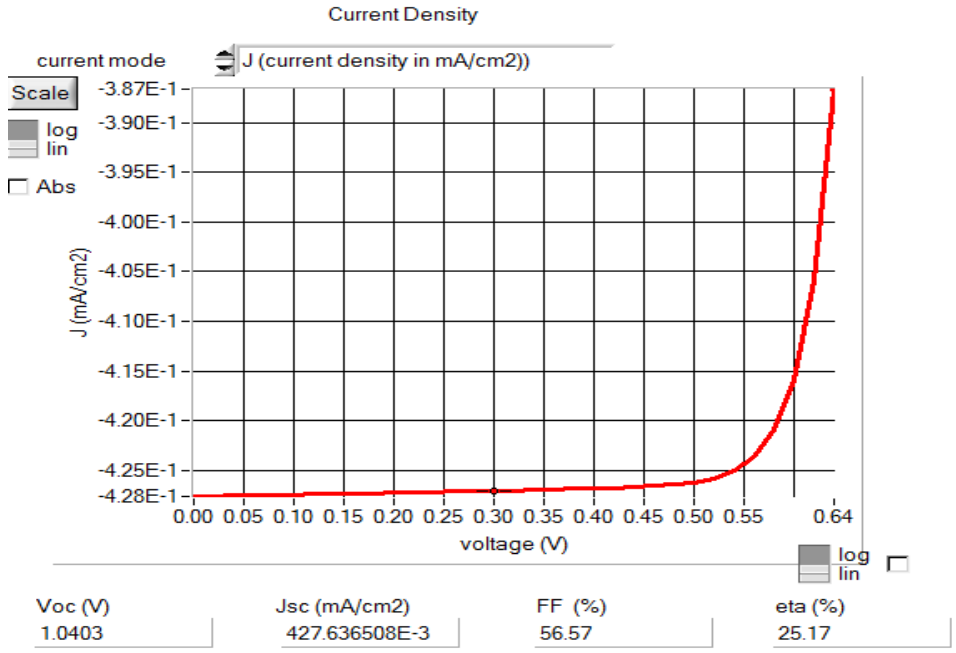

Figure: 3-27 J_{SC} and V_{OC} of CIGS solar cell with ZnS buffer layer of .1um thickness and corresponding efficiency

Cell efficiency fell over 1% by doubling the thickness of ZnS. As stated previously, ZnS has a band gap of 3.68 eV. From sweeping figures, ZnS reached peak efficiency at 0.04µm. Increasing the thickness efficiency began to fall off.

Table: 3-15 Comparison of I-V characteristics, fill factors and efficiencies w.r.t ZnS thickness

	0.04um	0.05um	0.06um	0.07um	0.1um
J_{SC} (mA/cm2)	0.434	0.431	0.428	0.428	0.427
V_{OC} (V)	1.4688	1.1212	1.0502	1.0424	1.0403
FF (%)	40.98	52.73	56.11	56.48	56.57
n (%)	26.15	25.51	25.27	25.23	25.17

3.4.3.3 Quantum Efficiency:

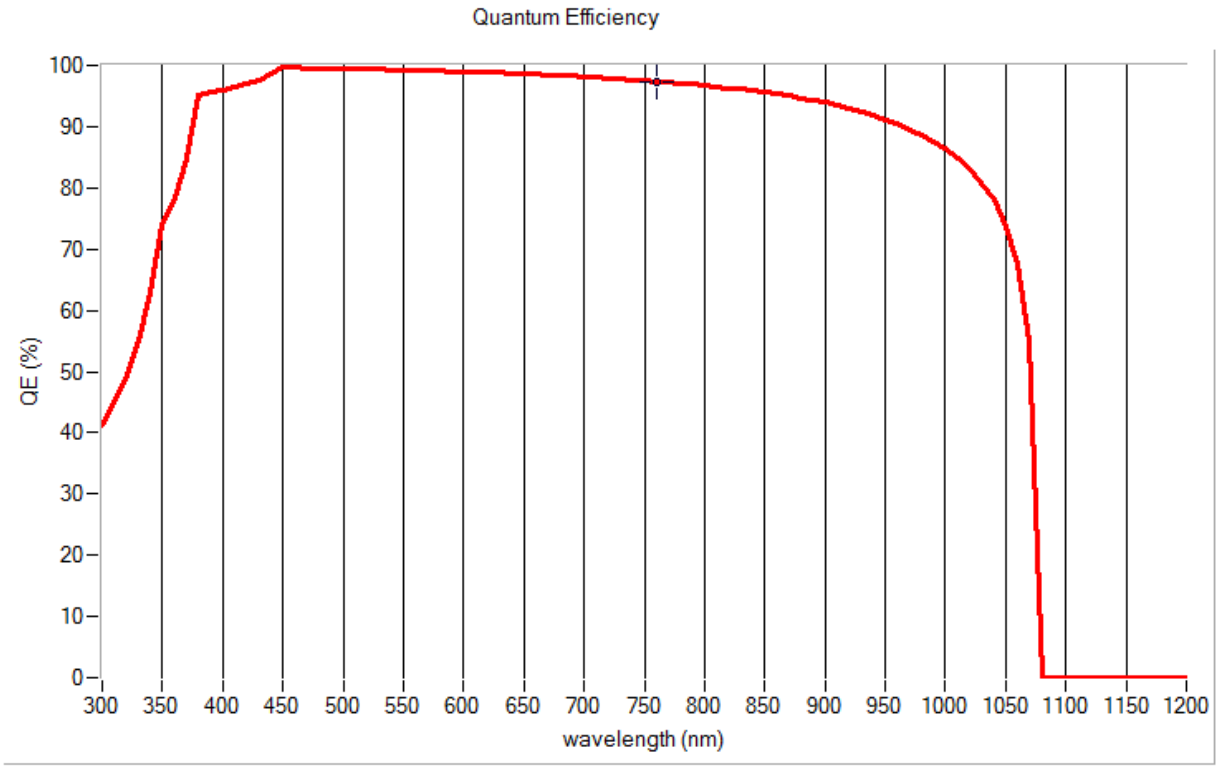

Figure: 3-28 Quantum efficiency of CIGS Solar cell with ZnS buffer layer

The external quantum efficiency of a solar cell is shown in Figure: 3-28. The spectral response curve shows a decrease of the long wavelength collection. This is most likely due to incomplete absorption of the long wavelength photons.

For ZnS buffer layer the maximum efficiency occurred from 400nm-750nm. The efficiency begin to fall off after 800nm.

3.5 Comparison between different buffer layers:

In this thesis, the thickness of buffer layer is optimized at 0.05um (nm), thicknesses less than 40nm currently is not reachable because of fabrication techniques and instruments limitation. Thus, the range of 40nm to 50nm is the preferred and the optimized thickness of the buffer layer in CIGS-based solar cell.

Table: 3-16 Semiconductor parameters of different buffer layers

Parameters	CdS	In_2S_3	ZnS
Bandgap (eV)	2.4	2.1-2.5	3.68
Electron Affinity (eV)	4.2	4.45	4.13
Dielectric Permittivity	10.0	13.6	8.9
CB effective density of states (1/cm3)	2.2E+18	1.8E+19	2.2E+18
VB effective density of states (1/cm3)	1.8E+19	4.0E+13	1.8E+19
Electron Thermal velocity (cm/s)	3.1E+7	1.0E+7	1.0E+7
Hole Thermal velocity (cm/s)	1.6E+7	1.0E+7	1.0E+7
Electron mobility (cm2/Vs)	1.0E+2	4.0E+2	2.5E+2
Hole mobility (cm2/Vs)	2.5E+1	2.1E+1	7.0E+1

3.6 Efficiency comparison:

The optimized data of corresponding different buffer layers is shown below:

Table: 3-17 Efficiency obtained with different buffer layers

	CdS	**In_2S_3**	**ZnS**
J_{SC} (mA/cm2)	0.460	0.387	0.431
V_{OC} (V)	0.6406	1.4428	1.1212
FF (%)	80.54	41.85	52.73
n (%)	23.74	23.39	25.51

From the optimized data, it is shown that when the CIGS solar cell is optimized with cadmium sulfide (CdS) buffer layer the maximum efficiency obtained is 23.74% with 0.05um buffer layer thickness. When the cell is optimized with Indium Sulfide (In_2S_3) buffer layer of 0.05um thickness, the maximum cell efficiency obtained is 23.39%. And highest efficiency is obtained with Zinc Sulfide buffer layer of 0.05um, which is 25.51%.

Chapter-4

CONCLUSION

4.1 Conclusion

The objective of this thesis was to design CIGS solar cells that were optimized for a specific climate or region. SCAPS was used as a virtual fabrication and modeling tool. A base line cell was created by entering the parameters and characteristics of other known CIGS cells to verify the validity of the model. Continuing from the base cell, four additional cells were created in which only the bandgap of CIGS layer (1.04ev, 1.15ev, 1.24ev, 1.41ev, 1.55ev) was varied by varying the Ga content. This yielded efficiency of 15.37%, 20.03% e, 23.74%, 26.31%, and 26.92% respectively. But practically it is difficult to obtain such large bandgaps of 1.41eV and 1.55eV for CIGS absorber layer. Therefore, the optimum value of badgap for CIGS absorber layer is 1.24eV. In this thesis another additional cells were created varying the thickness of CIGS by 1um, 1.5um, 2um, 2.5um which gives the efficiency of 21.65%, 22.61%, 23.74%, 24.63% respectively keeping the bandgap constant. This research focused on optimizing the thicknesses of the semiconductor layers in each of the band gap cells. The semiconductor layers that were optimized were Al:ZnO-0.2 µm, iZnO-0.1 µm, CdS/In_2S_3/ZnS-0.05 µm, CIGS-2.0 µm, and Mo-0.4 µm.

In this investigation, the CdS buffer layer is replaced by other materials like Zinc Sulphide (ZnS) and Indium Sulphide (In_2S_3). We concluded that ZnS can be used as alternative material to CdS. We calculated the efficiency of CIGS solar cell using different buffer layer e.g. In_2S_3, ZnS, CdS. Each of the buffer layer was varied by thickness of 0.04um, 0.05um, 0.06um, 0.06um, 0.07um, 0.1um and corresponding efficiency was calculated. Here we observed that efficiency increased by decreasing the thickness of buffer layer. The highest efficiency was found using ZnS is 25.51% with the thickness of 0.05um. The current world record efficiency for CIGS is 22.6%. While the efficiency in this thesis is only theoretical, it exceeds the current record efficiency by 2.91%. The solar spectrums of AM1.5 used for this simulation at 300k and 100 mW/cm2.

4.2 RECOMMENDATIONS FOR FUTURE WORK

1. Physical Confirmation of Model

Confirmation of the model was an important step in this research; however, it is not a sufficient substitute to physical validation. CIGS cells with varying band gaps and different buffer layers need to be produced and tested in contrasting geographic locations or solar irradiance to validate the concept presented in this thesis.

2. Model Improvement

Additional research is required in order to improve the SCAPS model used in this thesis. Research into how manufacturing defects affect the performance and how to model these characteristics will produce a more accurate model. Electron hole mobility and lifetime also need to be more accurately modeled for higher band gap CIGS material.

3. Currently Manufactured Cell Parameters

As stated before, current manufactures parameters for high efficient CIGS cells were not available. This is due to company's reluctance to freely publish parameters that required thousands of dollars and man hours to determine. By obtaining real world parameters, a more accurate model can be created and validated.

4. Additional Solar Spectrums

Designing solar cells that were specifically tuned to the solar irradiance of a region was investigated in this thesis. In order to fully validate this concept, additional solar irradiance profiles need to be entered into SCAPS. Currently, SCAPS contain the standard spectrums of AM0 and AM1.5. By entering measured solar irradiance into the model, a true optimum band gap cell can be developed and tested.

5. Higher Efficiency CIGS Concepts

With CIGS ability to vary band gap, differing designs could be tested in an attempt to achieve higher efficiency cells. A dual junction CIGS cell could be attempted by placing a higher band gap CIGS material above a lower band gap one. Another concept would be to design a CIGS layer that continually changed band gap with thickness. The top of the CIGS layer would be high band gap material and then gradually transition to lower band gaps towards the bottom of the cell. This gradient could possess the benefits of a multi-junction cell without the need for tunnel junctions between layers of different materials. Another approach can be taken by changing the window layer with transparent conducting oxide (TCO) which consist the properties to reduce the recombination losses.

This page is left intentionally blank

LIST OF REFERENCES:

1. Administration, U.S.E.I., *International Energy Outlook 2011*, 2011.
2. Murray, J. and D. King, *Climate policy: Oil's tipping point has passed.* Nature, 2012. 481(7382): p. 433-435.
3. Barnosky, A.D., et al., *Approaching a state shift in Earth/'s biosphere.* Nature, 2012. 486(7401): p. 52-58.
4. Group, E.W. *URANIUM RESOURCES AND NUCLEAR ENERGY*. 2006 3rd December 2006; Available from: http://www.energywatchgroup.org/fileadmin/global/pdf/EWG_Report_Uranium_3-12 2006ms.pdf.
5. Fairley, P., *Germany Folds on Nuclear Power*, in *IEEE Spectrum*2011.
6. http://www.firstsolar.com/Innovation/CdTe-Technology.
7. Outlook, W.E. *Access to Electricity*. Available from: http://www.iea.org/weo/electricity.asp.
8.3rdDecember,2017;http://ffden2.phys.uaf.edu/212_spring2011.web.dir/Elliot_Smith/history.html
9. Nelson, J., *The Physics of Solar Cells* 1ed. 2003: Imperial College Press.
10. Madan Morusu, Investigation of CZTSe Solar Cell with ZnS, ZnSe and In2S3 as Buffer Layers: p. 6-10
11. 10. www.nd.edu/~gsnider/EE698A/Yogesh_Solar_cells.ppt.
12. S. Michael, “Renewable energy at military bases and for the warfighter,” class notes for EC3240, Department of Electrical and Computer Engineering, Naval Postgraduate School, July, 2013.
13. PV Education.Org, PN Junction [Online]. Available: http://pveducation.org/pvcdrom/pn-junction/doping
14. Srinivas, B., Balaji, S., Nagendra Babu, M. and Reddy, Y.S. (2015) Review on Present and Advance Materials for Solar Cells. *International Journal of Engineering Research-Online*, **3**, 178-182.
15. Bertolli, M. (2008) Solar Cell Materials. Course: Solid State II. Department of Physics, University of Tennessee, Knoxville.
16. Saga, T. (2010) Advances in Crystalline Silicon Solar Cell Technology for Industrial Mass Production. *NPG Asia Materials*,
2, 96-102. http://dx.doi.org/10.1038/asiamat.2010.82
17. Jayakumar, P. (2009) Solar Energy Resource Assessment Handbook. Renewable Energy Corporation Network for the Asia Pacific.
18. Chopra, K.L., Paulson, P.D. and Dutt, V. (2004) Thin-Film Solar Cells: An Overview. *Progress in Photovoltaics*, 12, 69-92. http://dx.doi.org/10.1002/pip.541
19. Imamzai, M., Aghaei, M., Hanum Md Thayoob, Y. and Forouzanfar, M. (2012) A Review on Comparison between Traditional Silicon Solar Cells and Thin-Film CdTe Solar Cells.

Proceedings of National Graduate Conference (*Nat- Grad* 2012), Tenaga Nasional Universiti, Putrajaya Campus, 8-10 November 2012, 1-5.

20. Types of Solar Panels, Grein Energy. Published 22 April 2015.

21. Maehlum, M.A. (2015) Energy Informative The Homeowner's Guide To Solar Panels, Best Thin Film Solar Panels— Amorphous, Cadmium Telluride or CIGS? Last updated 6 April 2015.

22. Elsabawy, K.M., El-Hawary, W.F. and Refat, M.S. (2012) Advanced Synthesis of Titanium-Doped-Tellerium-Camium Mixtures for High Performance Solar Cell Applications as One of Renewable Source of Energy. *International Journal of Chemical Sciences*, 10, 1869-1879.

23. Bertolli, M. (2008) Solar Cell Materials. Course: Solid State II. Department of Physics, University of Tennessee, Knoxville.

24. Badawy, W.A. (2015) A Review on Solar Cells from Si-Single Crystals to Porous Materials and Quantum Dots. *Journal of Advanced Research*, 6**,** 123-132. http://dx.doi.org/10.1016/j.jare.2013.10.001

25. Hoppe, H. and Sariciftci, N.S. (2008) Polymer Solar Cells. *Advances in Polymer Science*, 214, 1.

26. Hoppe, H. and Sariciftci, N.S. (2008) Polymer Solar Cells. *Advances in Polymer Science*, 214, 1.

27. Choubey, P.C., Oudhia, A. and Dewangan, R. (2012) A Review: Solar Cell Current Scenario and Future Trends. *Recent Research in Science and Technology*, 4, 99-101.

28. Brabec, C.J., Shaheen, S.E., Winder, C. and Sariciftci, N.S. (2002) Effect of LiF/Metal Electrodes on the Performance of Plastic Solar Cells. *Applied Physics Letters*, 80, 1288. http://dx.doi.org/10.1063/1.1446988

29. Bagher, A.M., Vahid, M.M.A. and Mohsen, M. (2015) Types of Solar Cells and Application. *American Journal of Optics and Photonics*, 3, 94-113

30. Liang, M., Xu, W., Cai, F.S., Chen, P.Q., Peng, B., Chen, J. and Li, Z.M. (2007) New Triphenylamine-Based Organic Dyes for Efficient Dye-Sensitized Solar Cells. *The Journal of Physical Chemistry C*, 111, 4465-4472. http://dx.doi.org/10.1021/jp067930a

31. Philipps, S.P., Bett, A.W., Horowitz, K. and Kurtz, S. (2015) Current Status of Concentrator Photovoltaics (CPV) Technology. Report Version 1.2, Fraunhofer Institute for Solar Energy Systems (NREL), September 2015.

32. Shi, D., Zeng, Y. and Shen, W. (2015) Pervoskite/c-Si Tandem Solar Cell with Inverted Nanopyramids: Realizing High Efficiency by Controllable Light Trapping. *Scientific Reports*, **5**, Article No. 16504.

33. P. Reinhard, A. Chirila, P. Blosch, F. Pianezzi, S. Nishiwaki, S. Buecheler, and A.
N. Tiwari, "Review of progress toward 20% efficiency flexible CIGS solar cells and manufacturing issues of solar modules" in *IEEE J. Photovoltaics,* vol. 3, no. 1, pp. 572-580, 2013.

34. A. Kanevce, "Anticipated performance of Cu(In,Ga)Se2 solar cells in the thinfilm limit," Ph.D. dissertation, Dept. Physics, Colorado State Univ., Fort Collins, CO, 2007

35. *Encyclopedia of Alternate Energy*, s.v."Silicon" [Online]. Available: http://www.daviddarling.info/encyclopedia/S/AE_silicon.html
36. R. Noufi and K. Zweibel, "High efficiency CdTe and CIGS thin-film solar cells: highlights and challenges" in *Conf. Record of the IEEE 4th World Conf., Photovoltaic Energy Conversion,* Waikoloa, HI, 2006, pp. 317-320.
37. Solar World, Solar Energy 101, Making Solar Panels [online]. Available http://www.solarworld-usa.com/solar-101/making-solar-panels
38. Optics.Org. (2010 Nov. 01). Taiwan investors push Solarion to mass production [online]. Available http://optics.org/news/1/6/2
39. J. V. Coba, "Application of Copper Indium Gallium Diselenide photovoltaic cells to extend the endurance and capabilities of the Raven RQ-11b unmanned aerial vehicle," M.S. thesis, Dept. Elec. Eng., NPS, Monterey, CA, 2010.
40. National Renewable Energy Laboratory. National Center for Photovoltaics [online]. Available: http://www.nrel.gov/ncpv/
41. Barreau, N., Marsillac, S., & Berne, J. C. (2001). Optical properties of wide band gap Indium Sulphide thin film obtained by physical vapor deposition. *physica status solidi (A), 186*(1), 179-186.
42. D. Hariskos, S. Spiering, M. Powalla, "Buffer layers in Cu(In,Ga)Se_2 solar cells and modules," *Thin Solid Films*, vol.480–481, pp. 99– 109, 2005.
43. N. Barreau, S. Marsillac, J. C. Bernedeand Assmann L., "Evolution of the band structure of □-In_2S_3□3xO3x buffer layer with its oxygen content," *Journal of Applied Physics*, vol. 93, pp. 5456-5459, 2003.

This page is left intentionally blank

APPENDIX

About SCAPS

SCAPS is a one dimensional solar cell simulation program developed at the department of Electronics and Information Systems (ELIS) of the University of Gent, Belgium. Several researchers have contributed to it's development: Alex Niemegeers, Marc Burgelman, Koen Decock, Johan Verschraegen, Stefaan Degrave. SCAPS is originally developed for cell structures of the CuInSe2 and the CdTe family. Several extensions however have improved its capabilities so that it is also applicable to crystalline solar cells (Si and GaAs family) and amorphous cells (a-Si and micromorphous Si).

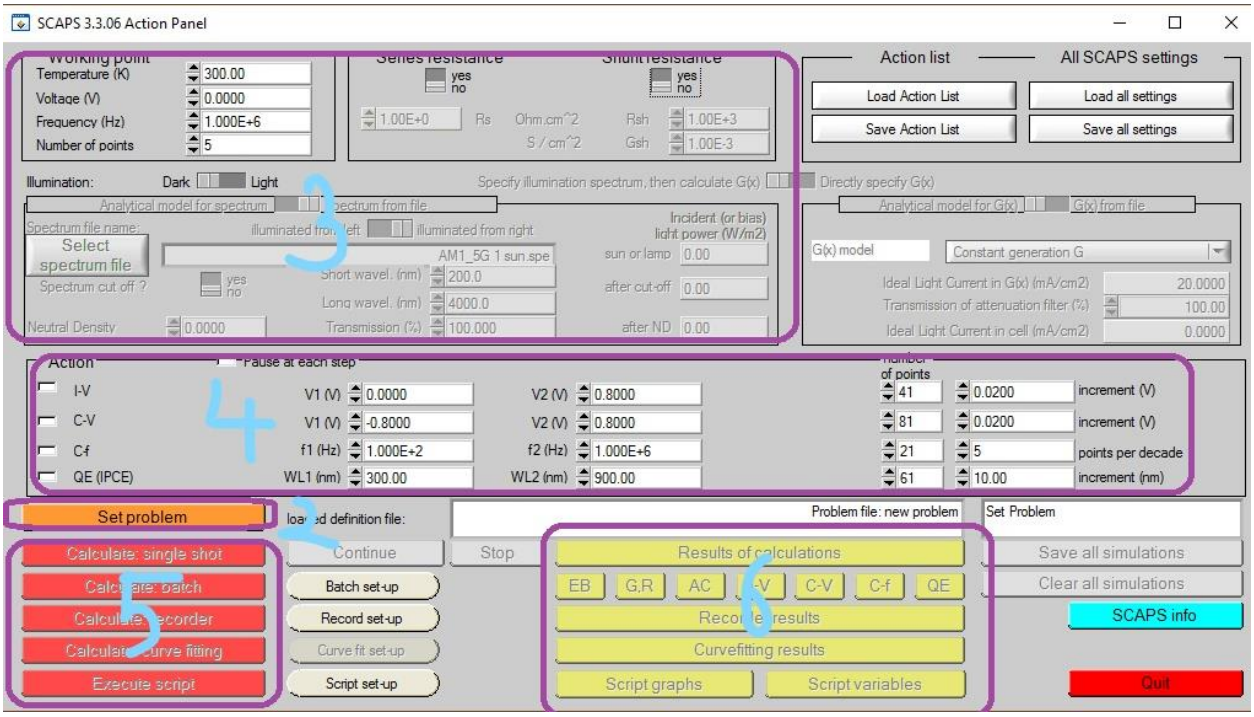

Figure : A-1 Action panel of SCAPS.

There are dedicated panels for the basic actions:

1. Run SCAPS .
2. Define the problem, thus the geometry, the materials, all properties of your solar cell
3. Indicate the circumstances in which you want to do the simulation, i.e. specify the working point

4. Indicate what you will calculate, i.e. which measurement you will simulate.
5. Start the calculation(s)
6. Display the simulated curves,

SCAPS is originally developed for cell structures of the CuInSe2 and the CdTe family. Several extensions however have improved its capabilities so that it is also applicable to crystalline solar cells (Si and GaAs family) and amorphous cells (a-Si and micromorphous Si). An overview of its main features is given below:

- up to 7 semiconductor layers
- almost all parameters can be graded (i.e. dependent on the ocal composition or on the depth in the cell): *Eg, χ, ε, NC, NV, vthn, vthp, μn, μp, NA, ND,* all traps (defects) *Nt*
- recombination mechanisms: band-to-band (direct), Auger, SRH-type
- defect levels: in bulk or at interface; their charge state and recombination is accounted for
- defect levels, charge type: no charge (idealisation), monovalent (single donor, acceptor), divalent (double donor, double acceptor, amphoteric), multivalent (user defined)
- defect levels, energetic distributions: single level, uniform, Gauss, tail, or combinations
- defect levels, optical property: direct excitation with light possible (impurity photovoltaic effect, IPV)
- meta-stable defects: transitions between acceptor and donor configurations for known meta-stable defects in CIGS: the V_Se and the In_Cu defect; also custom set meta-stable transitions implemented.
- contacts: work function or flat-band; optical property (reflection of transmission filter) filter
- tunneling: intra-band tunneling (within a conduction band or within a valence band); tunneling to and from interface states
- generation: either from internal calculation or from user suppied *G*(*x*) file
- illumination: a variety of standard and other spectra included (AM0, AM1.5D, AM1.5G, AM1.5Gedition2, monochromatic, white,...)
- illumination: from either the *p*-side or the *n*-side; spectrum cut-off and attenuation
- working point for calculations: voltage, frequency, temperature
- the programme calculates energy bands, concentrations and currents at a given working point, *J-V* characteristics, ac characteristics (*C* and *G* as function of *V* and/or *f*), spectral response (also with bias light or voltage)
- batch calculations possible; presentation of results and settings as a function of batchparameters

- loading and saving of all settings; startup of SCAPS in a personalised configuration; a script language including a free user function
- very intuitive user interface
- a script language facility to run SCAPS from a "script file"; all internal variables can be accessed and plotted via the script.
- a built-in curve fitting facility

Editing a solar cell structure

When clicking the ‘Set Problem’-button on the action panel, the ‘Solar cell definition’-panel is displayed. This panel allows to create/edit solar cell structures and to save those to or load from definition files. These definition files are standard ASCII-files with extension ‘*.def’ which can be read with e.g. notepad. Even though the format of these files seems self-explaining it is however strongly misadvised to alter them manually.

Device model

- Device is modeled in one dimension across layers, and formed junctions in physical space
- Depth is x coordinate
- Spatial distributions of fields, charge carriers, defect, etc.

Physics model: interfaces

- The quasi-fermi levels are allowed to be discontinuous at the interfaces.
- Recombination at the interface states is handled Example: recombination between electrons of CdS and holes in the CdTe on the right side of the interface.

Physics model: grading

- Almost all parameters can be graded; the principles of the algorithms used to simulate graded solar cell structures

• All parameters are consistently derived from the composition grading of a layer – Each layer is assumed to have composition A1-yBy – Define values of a parameter P for pure compounds A, B, and the composition grading y(x) over the layer thickness – Specify some grading law for P(y).

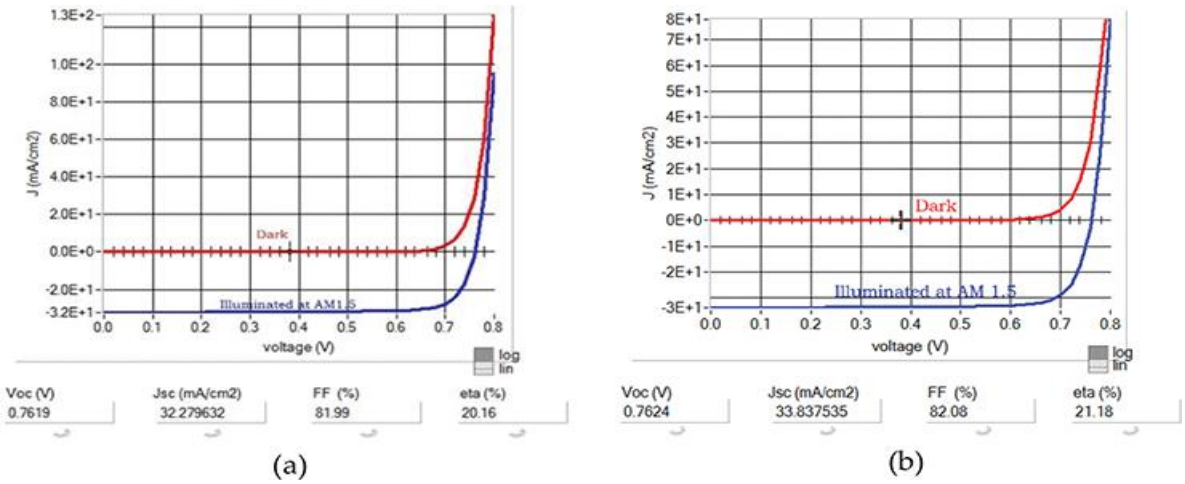

Figure: A-2 Grading in SCAPS.

Physics model: generation

• From internal calculation under illumination – Dark or light, power level (~ND filter), choice of the illuminated side, choice of the spectrum.

• From user supplied generation g(x) file, at the xcoordinates of the nodes used by SCAPS – allows for modeling of radiation detectors, EBIC measurements – Solar cell efficiency and QE cannot be calculated; may use collection efficiency, based on " ideal" device current.

Physics model: recombination

• Direct band-to-band – Between the occupied states in the CB and the vacant states in the VB.

• Indirect, or Shockley-Read-Hall – Through a defect state in the gap – Also through interface states.

• Auger recombination – Involves three carriers: after recombination, the energy is given an electron in the conduction band (as opposed to emission as a photon or phonon).

Output

• In each calculation the running parameter (V, f, or l) is varied in the specified range • Plot all calculated parameters, such as I/V, C/V, C/f, Q(l), band diagrams, concentrations, and currents • All calculations can be saved in ASCII format • When divergence occurs, the points calculated so far are shown on the corresponding graphs • Batch calculations possible; presentation of results and settings as a function of batch parameters.

Device definition

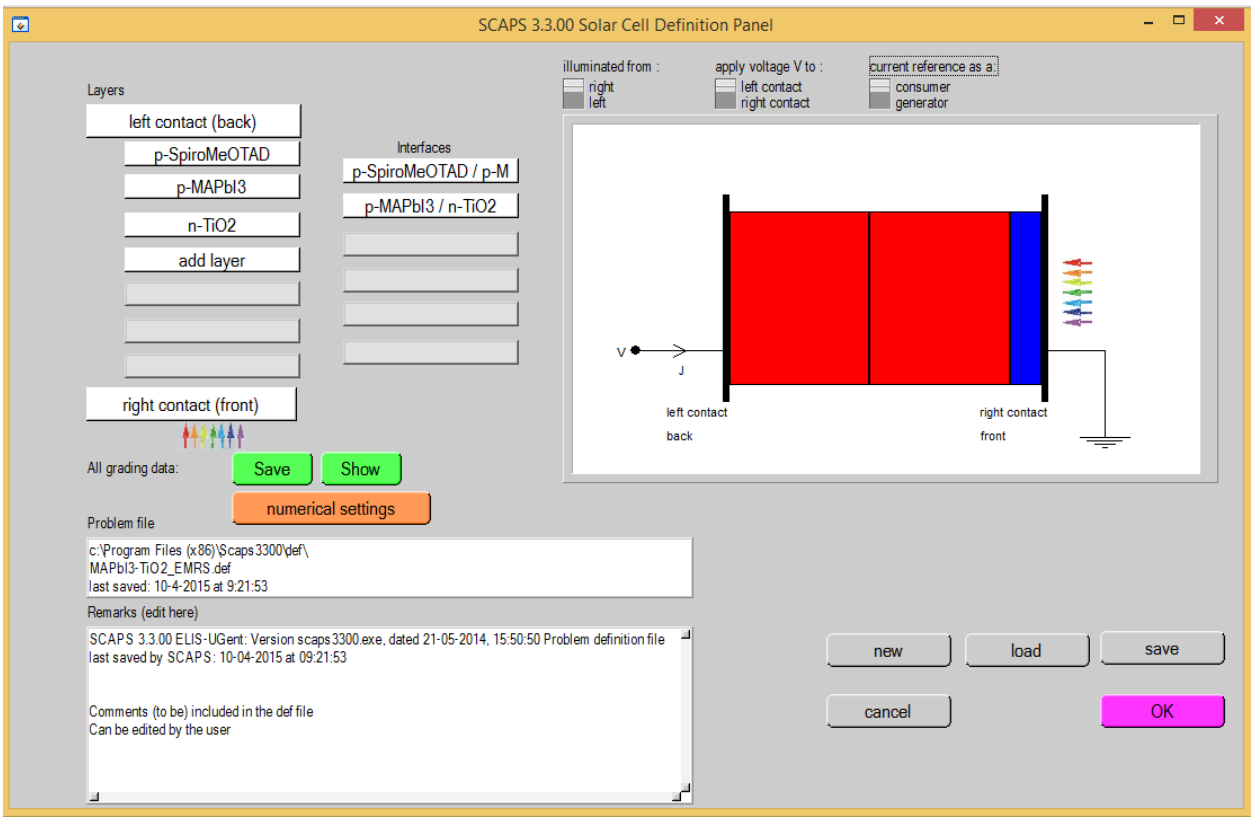

Figure: A-3 Solar cell definition panel in SCAPS.

• Device is represented as a stack of layers, up to 7 semiconductor layers with specified properties

• Separate entries for interface parameters

• Two additional layers for contacts, front and back .

Quantum efficiency

• The Q.E. is the ratio of the number of carriers collected by the solar cell to the number of photons of a given energy incident on the solar cell .

• If all photons of a certain wavelength are absorbed and the resulting minority carriers are collected, then the quantum efficiency at that particular wavelength is unity.

• The quantum efficiency for photons with energy below the band gap is zero.

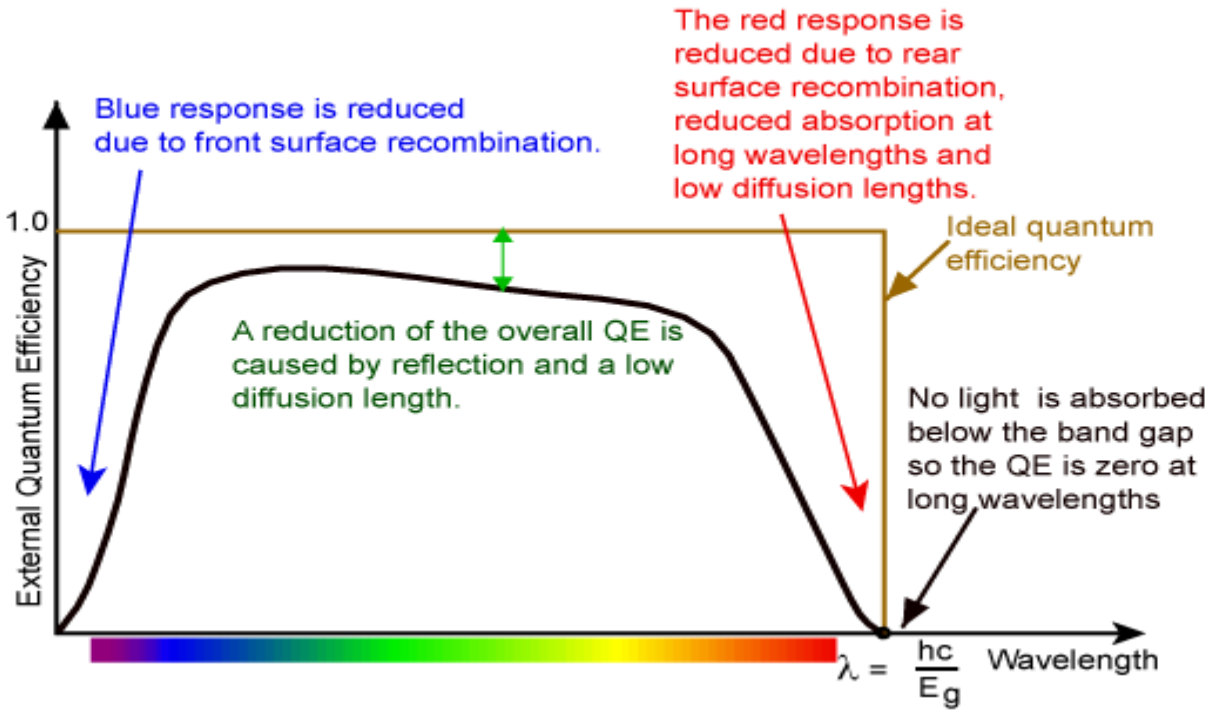

Figure: A-4 Quantum efficiency vs wavelength.

Summary

SCAPS-1D is a versatile package for semiconductor device modeling.

• Output for I/V, C/V, C/f, Q(I), band diagrams, concentrations, and currents.

• Data analysis for I-V, C-V, C-f.

• A number of standard models available with the distribution package.

• Well-developed user interface, convenient scripting facilities.